Available online at www.sciencedirect.com
ScienceDirect
Nuclear Engineering and Design 238 (2008) 1471–1495
Nuclear Engineering and Design
www.elsevier.com/locate/nucengdes

The MEGAPIE-TEST project: Supporting research and lessons learned in first-of-a-kind spallation target technology

C. Fazio [a,*], F. Gröschel [b], W. Wagner [b], K. Thomsen [b], B.L. Smith [b], R. Stieglitz [a], L. Zanini [b], A. Guertin [c], A. Cadiou [c], J. Henry [d], P. Agostini [e], Y. Dai [b], H. Heyck [b], S. Dementjev [b], S. Panebianco [d], A. Almazouzi [f], J. Eikenberg [b], A. Letourneau [d], J.C. Toussaint [d], A. Janett [b], Ch. Perret [b], S. Joray [b], J. Patorski [b], W. Leung [b], P. Meloni [e], P. Turroni [e], A. Zucchini [e], G. Benamati [e], J. Konys [a], T. Auger [g], A. Gessi [e], D. Gorse [g], I. Serre [h], A. Terlain [d], J.-B. Vogt [h], A. Batta [a], A. Class [a], X. Cheng [a], F. Fellmoser [a], M. Daubner [a], S. Gnieser [a], G. Grötzbach [a], R. Milenkovic [a], C. Latgé [d], J.U. Knebel [a]

[a] *Forschungszentrum Karlsruhe GmbH, P.O. Box 3640, 76021 Karlsruhe, Germany*
[b] *Paul Scherrer Institut, 5232 Villigen PSI, Switzerland*
[c] *SUBATECH Laboratory, CNRS/IN2P3-EMN-University, F-44307 Nantes, France*
[d] *Commissariat à l'énergie atomique, 91191 Gif-sur-Yvette Cedex, France*
[e] *Ente per le nuove Tecnologie, l'Energia e l'Ambiente, Località Brasimone, 40032 Camugnano, Bologna, Italy*
[f] *Studiecentrum voor Kernenergie/Centre d'Etude de l'Energie Nucléaire, Boeretang 200, 2400 Mol, Belgium*
[g] *CNRS-CECM, 15 rue Georges Urbain, 94407 Vitry/Seine Cedex, France*
[h] *CNRS-LMPGM, 59655 Villeneuve d'Ascq Cedex, France*

Received 20 April 2007; received in revised form 10 September 2007; accepted 5 November 2007

Abstract

The megawatt pilot experiment (MEGAPIE) has been launched by six European institutions (PSI, FZK, CEA, SCK-CEN, ENEA and CNRS), JAEA (Japan), DOE (US) and KAERI (Korea) with the aim to carry out an experiment, in the SINQ target location at PSI (Switzerland), to demonstrate the safe operation of a liquid metal (lead–bismuth eutectic, LBE) spallation target hit by a ~1 MW proton beam. The European Commission has joined the MEGAPIE project through the 5-year (2001–2006) project named MEGAPIE-TEST. This project has been formally concluded with an International Workshop, where the results and the lessons learned during the project have been summarised. This work presents a review of the outcome of that Workshop.

1. Introduction

The MEGAPIE-TEST project has been supported by the European Commission in the frame of "Partitioning and Transmutation" activities foreseen in the component of "Safety of the fuel cycle" belonging to the key action "Nuclear Energy" of the 5th Framework Programme. The Project has been formally concluded with an International Workshop where the most relevant results gained during the project have been discussed. The summary of these results is reported in this work.

The partitioning and then the transmutation of the Minor Actinides (Am, Np and Cm) present in the spent nuclear fuel as unloaded from nuclear power plants provides a potential tool to reduce the burden on a deep geological repository (Salvatores, 2005). Accelerator Driven sub critical Systems (ADS) have been proposed to transmute Minor Actinides (European TWG on

* Corresponding author.
E-mail address: concetta.fazio@nuklear.fzk.de (C. Fazio).

0029-5493/$ – see front matter © 2007 Elsevier B.V. All rights reserved.
doi:10.1016/j.nucengdes.2007.11.006

ADS, 2001). In these systems, a spallation target located inside a sub-critical fast neutron reactor core provides the external source of neutrons, as needed for a stable operation.

The neutrons are produced via spallation reaction of a high power proton beam colliding with the material of the target. The power of the beam and the specific target material, define important characteristics of the ADS. For instance a 1–2 MW_{th} spallation heavy liquid metal (HLM) target would be required to provide the external source for a sub-critical system having a k_{eff} between 0.95 and 0.98 and a core power between 50 and 100 MW_{th} (Salvatores et al., 1994).

In fact, in order to get strong neutron sources, the use of HLM as spallation materials has been envisaged. However, an HLM target to be irradiated in a high intensity proton beam has never been built. Moreover, it has been generally recognized that the spallation target is an innovative and most challenging component of an ADS, itself an innovative concept which would need a detailed experimental validation. Therefore, an international initiative (the MEGAPIE, megawatt pilot experiment) has been launched in 1999 to build and operate a representative (in terms of power and target material) spallation target, to be realized in the SINQ facility at PSI. The accelerator feeding the SINQ facility, as described with more details in Section 2, delivers a proton beam of about 590 MeV and a current up to 2.0 mA with a total proton beam power of about 1.18 MW.

After an initial feasibility study, performed by the MEGAPIE consortium (Bauer et al., 2001), the conceptual design of the target and of its ancillary systems (i.e. heat removal system, cover gas system, fill and drain system and the insulation gas system) has started. The design team was supported by multi-laboratory R&D groups active in the areas of neutronics and nuclear assessment; thermal-hydraulics and structure mechanics; materials and liquid metal technologies. The conceptual design was adapted to the SINQ boundary conditions (e.g. beam entrance from the bottom) and supported by the results obtained by the R&D groups. For instance, the beam power deposition profile, calculated with the MCNPX (Waters et al., 2002) and FLUKA (Fassò et al., 2001) codes, has been used to design and study the overall coolability and the structural integrity of the target and its interface (window) with the proton beam, and validation experiments have been performed. Similarly, the isotope production calculations made with MCNPX and FLUKA, have been used to design the cover gas system. As for the selected structural materials (ferritic/martensitic 9Cr "T91" and the austenitic "AISI 316L" steels), they have been assessed in terms of corrosion and irradiation performances under MEGAPIE relevant conditions using specific experiments. Details on the R&D results in the different areas are described in Section 4.

Beam monitoring and HLM leak detection systems have also been the subject of relevant R&D efforts. These topics will be discussed in Section 6.

After having fixed the conceptual design of the target and the ancillary systems, which are described in Sections 3 and 5 respectively, the project entered in the engineering design and the manufacturing phases, within a strict Quality Assurance scheme to comply with Swiss nuclear requirements.

Single components, as the Electromagnetic Pump System, the beam entrance window and the cooling pin of the heat exchanger have been built first as prototype and tested in order to assess their performances. The target and its ancillary systems have been integrated and tested out-of-beam in the so-called MEGAPIE Integral Test Stand (MITS). The objectives of the MITS experiments were to first integrate all systems, to check their functionality by simulating normal operating conditions and transients (e.g. beam trips, beam interruptions, loss of coolant) postulated for the MEGAPIE target in SINQ. The results of the single component tests have been combined with the results obtained at the MITS to assess the overall target performance, as described in Section 7.

Finally, parallel to the design phase, the safety report has been prepared and submitted to the Swiss Federal Office of Public Health (BAG) to start the licensing procedure for the irradiation of the MEGAPIE target (Section 8). After having satisfied all requirements asked by the BAG (e.g. demonstration of a viable solution to protect SINQ against fire risk due to the selection of the organic oil as secondary coolant and the demonstration that an all encompassing reference accident case as defined by the BAG could be mastered), the target and the ancillary systems have been dismounted from the MITS and remounted in the SINQ target location. In this position all systems have been rechecked before starting the irradiation phase.

First protons have been sent on the target on August 2006 and the irradiation procedure, as described in Section 9 has been followed, before ramping the proton beam up to maximum power. The target has been successfully irradiated (between August 2006 and December 2006) up to an accumulated charge of 2.8 A h and with an availability of the order of 95%. The objective to design, manufacture and safely operate a heavy liquid metal spallation target has been therefore effectively fulfilled.

2. The Swiss spallation neutron source SINQ

The Swiss Spallation Neutron Source SINQ is operated at the Paul Scherrer Institute (PSI), driven by PSI's proton accelerator complex, a cascade of three units, the Cockroft-Walton pre-accelerator (860 keV), the Injector Cyclotron 2 (72 MeV) and the main Ring Cyclotron, the latter accelerating the protons to a final energy of 590 MeV. The cyclotrons operate with a radio frequency (rf)-bunch structure of 51 MHz. For the spallation reaction this is an essentially continuous (cw)-beam, making SINQ a *continuous* spallation neutron source. At present this accelerator is capable to deliver a stable proton current of 1.8–2.0 mA, equivalent to a maximum power of 1.18 MW. After having passed two graphite targets for meson production, Target M and Target E, about 1.3 mA of the primary proton beam reach the SINQ spallation target. Thus, receiving routinely up to 0.75 MW beam power, SINQ is presently the most powerful spallation neutron source worldwide.

The SINQ target location is an about 5 m long slim space where the target is inserted from the top into the massive target shielding block. The proton beam is entering the target vertically bottom-up, whereas all connections and supplies must enter from the top through the target head. These boundary con-

ditions imposed very restrictive requirements on the geometry and design of the MEGAPIE target. Likewise, they make the target head enclosure chamber (TKE) the essential location to provide all supplies necessary to operate the target. In particular for MEGAPIE the main ancillary systems, like the heat removal system, cover gas system and fill and drain system, had to find place in the rather narrow-spaced TKE, a challenging task on its own.

3. Target design and manufacturing

The target has been designed to accept a proton current of 1.74 mA. The thermal energy deposited in the lower part of the target is removed by forced convection. LBE is driven by the main inline electromagnetic pump, and then passes through a 12-pin heat exchanger (HX) and return to the spallation region. The heat is evacuated from the heat exchanger through a diathermic oil loop to an external intermediate water cooling loop and then finally goes into the PSI existing cooling system. The beam entrance window is cooled both by the main flow and also by a cold LBE jet extracted at the heat exchanger outlet, which is pumped by a second electro magnetic pump. The target has been conceived in nine sub-components, which were manufactured separately and finally assembled:

- The central rod (CR), inserted in the upward LBE flow path, includes a 20 kW heater and micro-fission chambers as neutron flux meters.
- The main flow guide tube which represents the barrier between the rising and down coming LBE flow. The guide tube is equipped with a number of thermo-couples to monitor the temperature field above the spallation zone.
- The electromagnetic pump system (main and by-pass) and flow-meters.
- The heat exchanger.
- The lower liquid metal container (LLMC). The target window is hemispherical with a wall thickness tapered from 1.5 mm in the centre to 2 mm at the outer rim.
- The lower target enclosure (LTE), a double walled, D_2O cooled hull, which is designed to contain any leakage. The reversed spherical shape of the LTE has been adopted to allow the LBE, in case of a leak, to flow into the lower edges of the LTE and avoid accumulation in the centre where the beam hits the target. The proper functioning of the LTE has been assessed by FEM calculations (Dury, 2003a,b) and dedicated experiment (Samec, 2006).
- Upper target enclosure (UTE). The UTE main function is to contain the insulation gas, and in case of accident to resist to overpressure and eventual mechanical shocks.
- Target head (TH) consisting of the main flange, which positions the target on the support flange of the central tube of the SINQ facility. All supplies to the target and instrumentation lines are fed through the target head.
- Target top shielding, which connects the LBE container to the target head. The LBE containing part of the target is thus suspended to the target head and allowed to expand freely. The component also contains tungsten to shield the target head area from the intense radiation of the LBE and the noble gases and volatiles collected in the gas expansion tank.

Table 1
MEGAPIE target main properties

Main specifications	
Length (m)	5.35
Weight (t)	1.5
LBE volume (l)	89
Gas expansion volume (l)	2
Gas pressure (bar)	0–3.2
Design pressure (bar)	16
Design temperature (°C)	400
Insulation gas (bar He)	0.5
Materials	
Lower liquid metal container	T91 ferritic/martensitic
Upper container	AISI 316L austenitic steel
Lower target enclosure	AlMg3
Heat removal and beam window cooling	
Deposited heat (kW)	700
Main pump (l/s)	4
Bypass pump (l/s)	0.35

The main characteristics of the MEGAPIE target are reported in Table 1 and a schematic view of the target is shown in Fig. 1.

The Target has been manufactured by ATEA REEL in France. Manufacturing, which lasted for 3 years, has been performed in close collaboration with PSI and SUBATECH. Prior to manufacturing, detailed design reviews were made to determine if a Lot was sufficiently defined to be manufactured (verification of

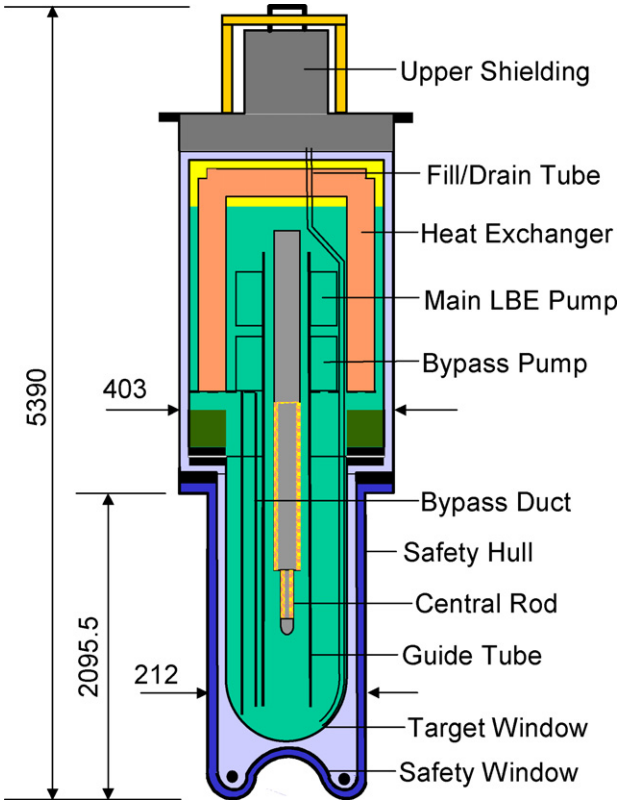

Fig. 1. Schematic of MEGAPIE target assembly.

the drawings, engineering and design documents). Step by step open design issues were solved and integrated in the drawings to come up with a final set of drawings for the manufacturer. A series of design calculations were performed to backup the target design. The readiness for manufacturing review was made to evaluate systematically one sub-component set of documents (general specifications, particular quality assurance program, drawing set, detailed specifications, engineering and design documents, manufacturing and sub-assembly plan, test inspection plan, schedule, cost update).

4. R&D support to the target design

4.1. Neutronic and nuclear calculations

The main tools used during the design phase for the neutronic and nuclear assessment of the MEGAPIE target were Monte Carlo transport codes. Important quantities such as neutron fluxes, power deposition in the target, shielding, dose rates, activation, gas production, and radiation damage, were calculated and the effects of the target design on the nuclear performance were evaluated. Clearly the input of the neutronic calculations is essential for instance for the design of the target beam window, for the target shielding, and for the handling procedure after irradiation.

The work followed several steps: first, a benchmark of the most widely used Monte Carlo codes, to perform a code intercomparison (Enderlé and Klein, 2001). The benchmark led to the choice of the FLUKA and MCNPX codes for the successive work.

Second, the two codes were used for the neutronic design of the target. The details of the neutronic design work are reported in Zanini (2005) and Zanini et al. (2005) and references therein. Then, a third phase started with the neutronic measurements and gas production, with the irradiation of the target. In this phase, the code predictions are validated, and the target performance is evaluated, first results are reported in Section 9 of this work.

4.1.1. Target performance

A comparison between the neutron flux with MEGAPIE and the SINQ solid target showed that the MEGAPIE target would deliver 40–50% more thermal neutrons to the instruments served by SINQ as compared to the SINQ solid target. It must be noted that the calculations of the solid target referred to an "ideal" case with the rods completely filled with Pb (while in reality 90% of the volume is filled) and without the STIP samples.

4.1.2. Power deposition

Approximately, 85% of the beam power is dissipated in the target-moderator system (71% in the LBE), the rest is dissipated in the surrounding shielding. Detailed beam power deposition on the structural materials was calculated. In particular, in the T91 beam window 1% of the total power is deposited. Despite this low power deposited it results in an unacceptably high increase in temperature which required an adequate cooling system. The calculated power deposition profiles in the target windows are shown in Fig. 2, as well as the graphic representation of the proton beam on the target.

4.1.3. Inner neutron flux assessment by means of innovative fission chambers

The inner neutron flux was assessed showing strong thermal/epithermal dependence as a function of the distance from the spallation zone. This ratio highly affects the activation of the target, having a great impact on the handling procedure.

To validate simulations and to measure the thermal/epithermal ratio, a neutron detector was designed (Chabod et al., 2006). It was composed by eight fission chambers imbedded in pairs along the axis of the detector. Each pair, except one, was made of a chamber containing ^{235}U fissile isotope and a chamber without deposit to compensate the fission signal from leakage currents or from currents induced by radiation fields. The bottom pair was shielded with natural gadolinium filter to absorb thermal neutrons and be more sensitive to epithermal neutrons. Finally, one pair was made of a chamber with ^{241}Am to measure the high-energy part of the flux and the other one

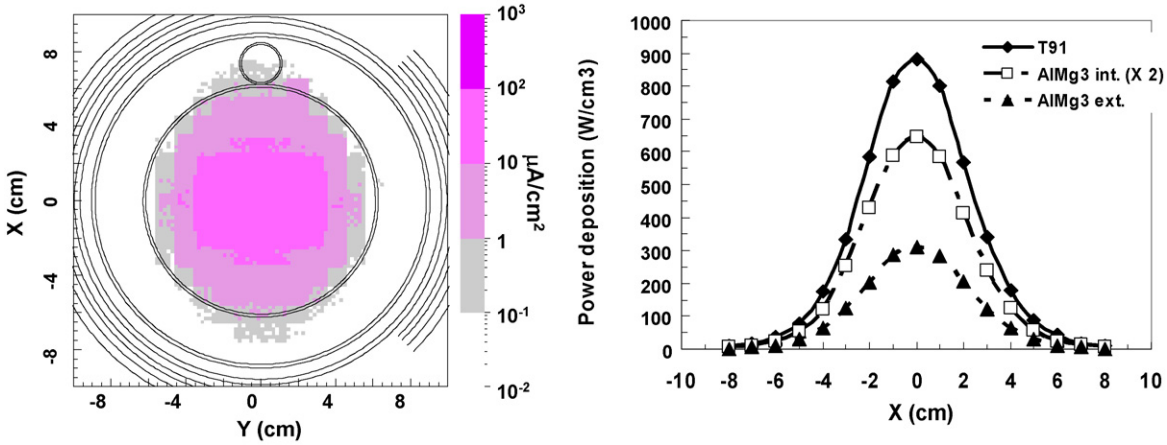

Fig. 2. (Left) Simulated proton beam on the target. The Gaussian profile follows calculations data from (Rohrer, 2001), giving a maximum current density of 30 μA/cm^2. (Right) Calculated power deposition in the target windows ($AlMg_3$ and T91) as a function of the x-axis ($y = 0$ cm) for a beam intensity of 1.74 mA. The curve for the $AlMg_3$ internal window is multiplied by 2 for visual identification.

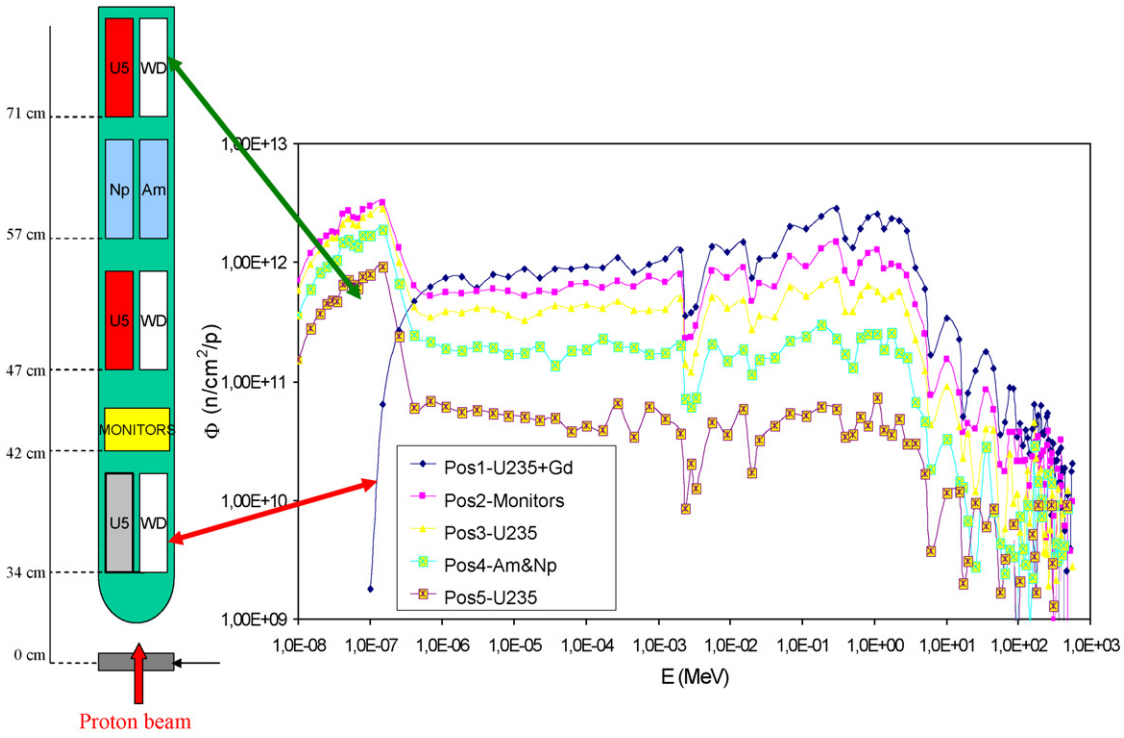

Fig. 3. Schematic view of the neutron detector with the corresponding simulated neutron spectrum.

with ^{237}Np to probe its incineration. These different configurations were chosen to provide an overall characterisation of the inside neutron flux, in terms of its intensity but also its energy distribution. To increase the accuracy on the energy spectrum determination, nine activation neutron flux monitors were put inside the detector in a small Ti-box. A schematic view of the positioning of the detectors and the corresponding simulated spectra is shown in Fig. 3. These monitors will be analyzed during the post-irradiation phase.

4.1.4. Isotope production

A comprehensive study of isotope production was undertaken, and several related topics were addressed: target activation and dose rates, radiation damage on the structural materials, gas production during irradiation and subsequent handling.

Prior to MEGAPIE irradiation, experimental effort was devoted to the measurement of the production rates of volatile elements on a proton irradiated LBE target (Zanini, 2005). This experiment was performed at the ISOLDE facility at CERN. Results were obtained for isotopes of several elements including He, Ar, Kr, Xe, I, Hg, and At isotopes. As an example, results for Xe isotopes, measured with the LBE target at $T = 600\,^{\circ}\mathrm{C}$, are shown in Fig. 4. Experimental results are compared with FLUKA and MCNPX calculations. In this case there is a clear disagreement between the values calculated with MCNPX with Bertini/Dresner, and the results from the other two calculations. It is assumed that at this temperature all the Xe is released but this will be confirmed by a post irradiation analysis of the target. Recent findings from thin target experiments agree with these results (Enqvist et al., 2001).

A third phase started with the neutronic measurements and of gas production, with the irradiation of the target. In this phase, the code predictions are validated, and the target performance is evaluated, first results are reported in Section 9 of this work.

4.2. Thermal-hydraulics and structure mechanics

Studies relating to the overall coolability and structural integrity of the lower target hull and safety vessel have been performed. Specifically, coolability relates to the efficient transport of heat from the heat-producing regions to the heat exchangers, and the protection of critical structures, particularly the beam

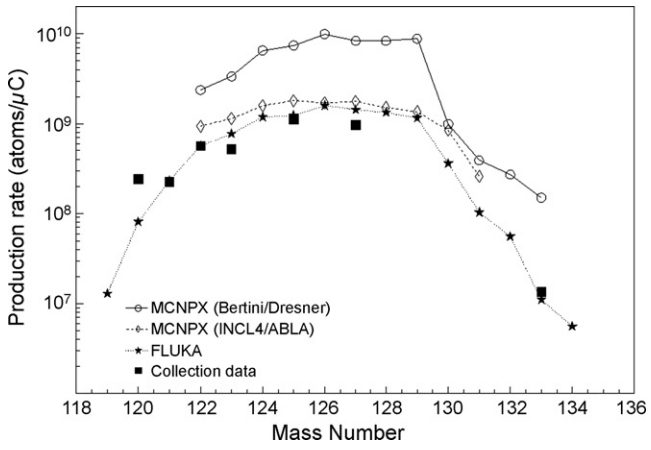

Fig. 4. Production rates for Xe isotopes. Measured points (black squares) are compared with calculations: open circles, MCNPX (Bertini/Dresner model combination); diamonds, MCNPX (INCL4/ABLA); stars, FLUKA.

window, from over-heating (local hot-spots) and excessive thermal gradients, which would result in high stress concentrations. However, it is not straightforward to verify the cooling principle by means of an integral test experiment, because of the difficulty of realistically reproducing the volumetric heating effect at representative power levels (1 GW/m^3) without actually using a beam. Consequently, the studies focused on the use of advanced numerical tools, both for the thermal hydraulics simulations and the associated structural analyses. A high level of confidence in these computations had to be demonstrated, and of necessity special-effects experimental tests using actual and simulant materials formed an integral part of the programme.

Considerable R&D was carried out to fulfil the project objectives. These being:

- to define the lower target flow configuration, within the geometric constraints imposed by the physical boundary conditions (geometrical confinement, LBE inventory, pump capacities, Heat Exchanger (HX) power, etc.);
- to identify, and evaluate, optimum target window design to minimize thermal loads and pressure drops, and to avoid hot-spots and flow instabilities;
- to demonstrate reliable cooling of the lower target enclosure (LTE);
- to demonstrate the structural integrity of the lower liquid–metal container (LLMC) and its internal components, and that of the LTE;
- to provide best-estimate safety margins on target coolability and structural integrity under operational flow conditions;
- to investigate, quantify, and make recommendations regarding, abnormal target operation (including possible accident scenarios).

Determination of the best-estimate steady-state beam footprint and axial heat deposition profile has been the subject of a neutronics benchmark exercise within the MEGAPIE project; see Section 4.1. Curve-fitting to the data has been carried out by Dury (2003a,b) and used for the CFD studies. The axial and radial heat deposition profiles in the LBE are shown in Fig. 5a. Beam orientation relative to the bypass nozzle can also be seen schematically in this sketch. For a proton beam current at the target of 1.74 mA (adopted for design studies), the total heat deposited in the target is about 700 kW.

4.2.1. Results of design studies

It was predicted (Zucchini and Smith, 2003b) that better window cooling and, particularly, less severe temperature differences (and associated stresses) in the lower part of the guide tube are obtained if the guide tube is slanted at the bottom (vertical distances to target hull 15 mm/25 mm or 10 mm/30 mm), with bypass flow on the large-gap side. The option 15 mm/25 mm was adopted for the target design to minimize risks of direct guide tube contact with the window under abnormal operating conditions. Following an in-depth CFD parameter study, a bypass mass flow rate of at least 2.5 kg/s (through a nozzle of cross-section about 200 mm^2, resulting in a discharge velocity of 1.2 m/s) was recommended to minimize window heating and maintain flow stability in the lower target region. This corresponds to a main mass flow rate of 37.5 kg/s.

The basic model (with the end of the guide tube not slanted) is shown in Fig. 6a. The position of the bypass channel is indicated in Fig. 6b, and two variants for the degree of slant of the end of the guide tube in Fig. 6c and d.

Typical velocities and temperatures obtained from the CFD are shown in Fig. 7. In the plane of the bypass flow, conditions are asymmetric, induced by the bypass jet and the guide tube slant. In the cross-plane, however, symmetric conditions prevail. The temperature distribution is quite non-uniform, ranging from 230 °C in the downflow annulus region, to over 380 °C in the LBE, just above the zone of beam heating. The important effect of the bypass flow (from the right) in providing a strong cross-flow over the window to enhance cooling is clearly seen in the figure.

Considerable work was done (Roubin, 2001, 2002, 2003a,b, 2004) to optimize the bypass nozzle shape and position. The critical parameters examined in this study were α, the angle the end of the nozzle makes with the horizontal (30° corresponds to a nozzle discharge that is initially parallel to the window surface), δ, the offset distance from the wall (see Fig. 8), and nozzle shape.

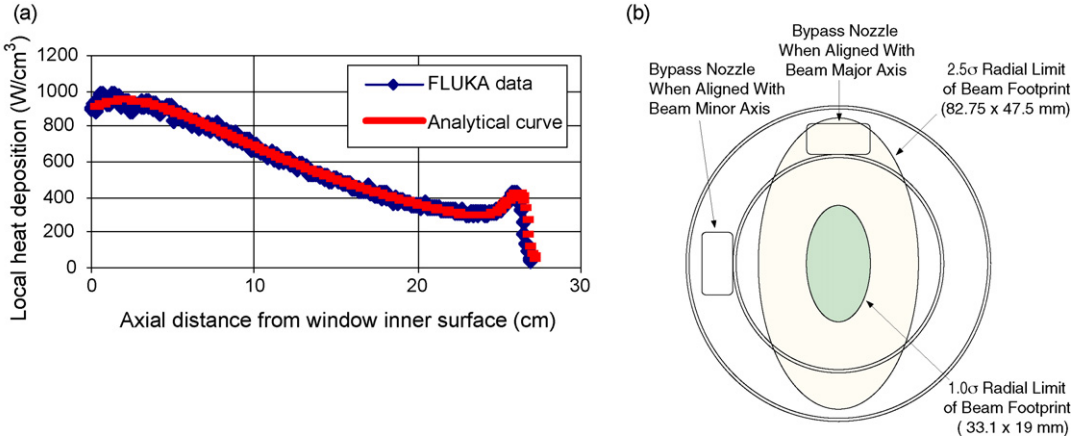

Fig. 5. (a) Axial heat deposition cure. (b) Beam footprint orientation relative to bypass nozzle.

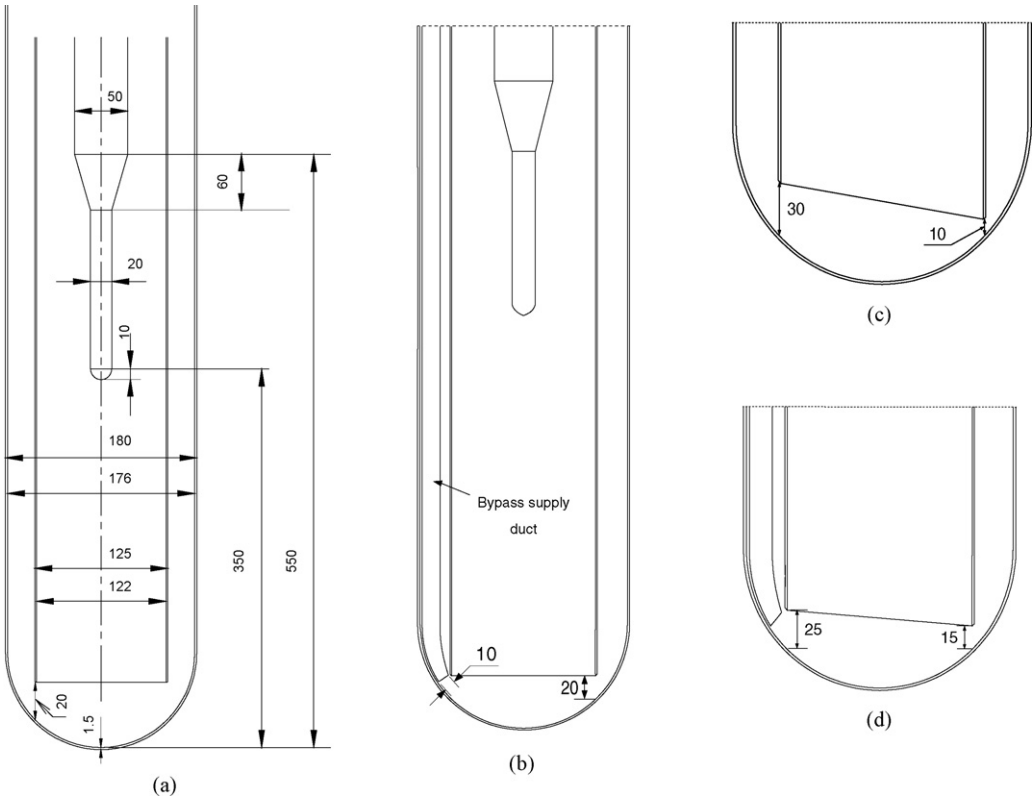

Fig. 6. Basic configuration of the CFD model, together with variants.

The following parameter options were investigated for three nozzle shapes (1) rectangular (20 mm × 10 mm); (2) weak elliptic (19.5 mm × 13 mm); and (3) strong elliptic (25.4 mm × 10 mm): $\alpha = 0°$, 15°, 30° and 40°; $\delta = 2.5$ mm and 5.0 mm.

CFD analyses confirmed the necessity of the bypass jet remaining attached to the window surface as the stream passes over the centre of the window, where the beam heating is greatest. The configuration $\alpha = 0°$, in which the bypass jet is directed vertically downwards, does not fulfil this requirement for the reference bypass flow rate of 2.5 kg/s.

For some parameter ranges (of main/bypass mass flow ratio), there was a strong sensitivity found to the position and orientation of the jet on whether the jet flow remained attached to the window or whether it detached. This feature has a strong influence on local window temperatures, since, with flow detachment, recirculation pockets are formed

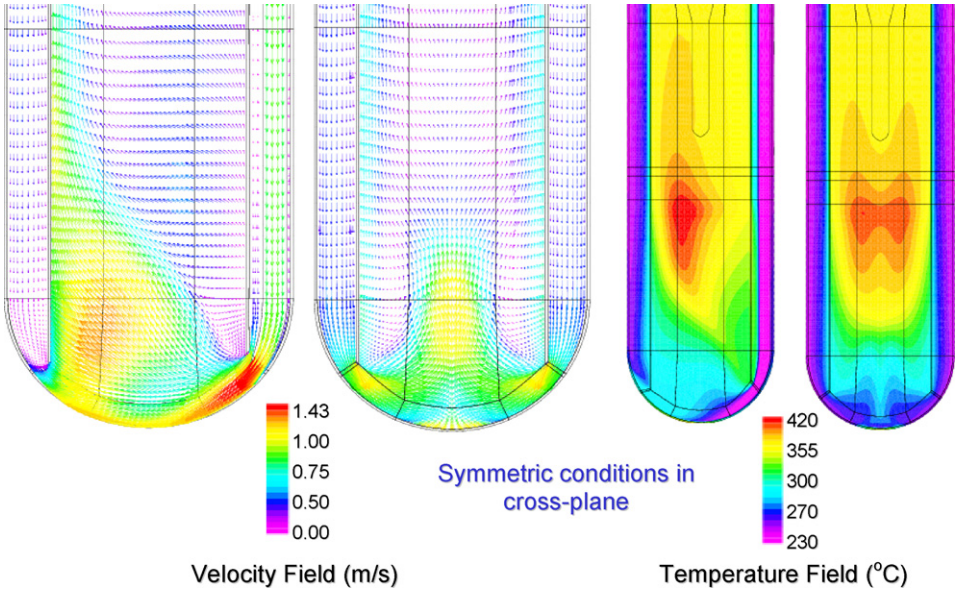

Fig. 7. LBE velocity and temperature fields in the plane of the bypass flow and cross-wise to it.

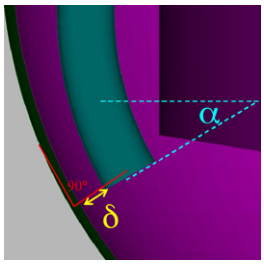

Fig. 8. Bypass nozzle optimization parameters.

from which heat is not very effectively removed. Best overall performance was obtained with the weakly elliptic nozzle (19.5 mm × 13 mm), located under the large-gap end of the guide tube, discharging at $\alpha = 15°$, and with a discharge mass flow rate of 2.5 kg/s. However, for ease of manufacture, a rectangular nozzle (20 mm × 10 mm) was adopted for the final target design.

Stress analyses were performed in combination with the CFD studies (Zucchini and Smith, 2003b). Of the lower-target components, stresses were greatest for the guide tube, caused by the differential heating in the riser. Detailed studies showed that spacers should be introduced to alleviate bending (Zucchini, 2002b). Stresses over the window were not severe (Fig. 9).

Similar studies (Smith and Shepel, 2005) were carried out for the lower target enclosure (LTE). These revealed that there was a very large safety margin on LTE coolabilty, with no serious hot spots or stress concentrations for steady-state operation with a D_2O flow rate of 2.2 kg/s. Finite Element Method (FEM) analysis of the "target catcher" ring has shown that the arrangement is effective in preventing contact of the LLMC and LTE in the event of total rupture of the target hull, and that stress levels at the supports can be tolerated (Samec, 2003).

4.2.2. *Operational transients*

Coupled CFD/FEM analyses have shown that, under normal operating conditions, maximum stress levels are kept within satisfactory limits: 46 MPa for the window and 49 MPa for the guide tube, with no increase of stresses during beam interrupt and restart events (Smith et al., 2005; Zucchini, 2005). Effects of beam wandering by up to 2 mm at the window were also investigated using CFD. It was shown that the maximum window temperature varies by only ±2 °C, and elsewhere by ±15 °C if the beam wanders off the central axis by these amounts (Smith, 2006).

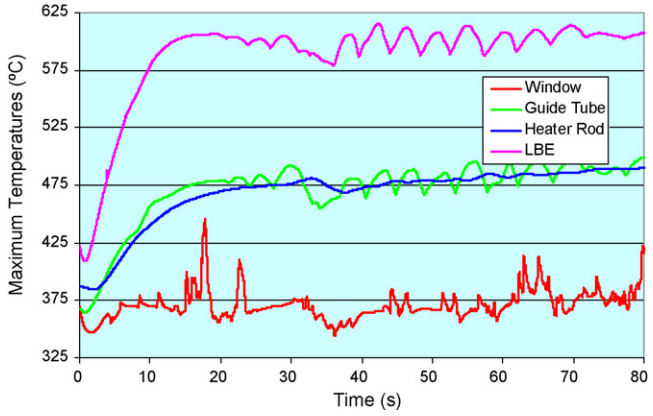

Fig. 10. Maximum temperature histories for the main-pump-failure transient.

4.2.3. *Abnormal and accident transients*

It is predicted that, with the slanted guide tube, there is sufficient cross-flow over the window to guarantee continued cooling in the event of failure of the bypass pump, though window temperatures increase sharply, and stresses reach 118 MPa (Smith et al., 2005). Likewise, it is predicted that the structural integrity of the LLMC would not be compromised if the main pump failed (Zucchini, 2005), since a reduced circulation would be maintained by natural circulation. However, as shown in Fig. 10, the flow field is not stable, and further operation of the target is not recommended (Leung, 2006).

Accidental over-focussing of the beam due to partial or total bypass of the scattering Target E has been identified as a serious event (Dury, 2003b). For beam focussing in excess of 35%, the window temperature does not stabilize, and structural failure can be anticipated (Zucchini and Smith, 2003a). Higher degrees of focussing reduce the time available to shut off the beam, and for 100% focussing this time reduces to 200 ms, imposing the installations of new safeguards and rapid-response detection devices (Section 6) for beam over-focussing prior to irradiation.

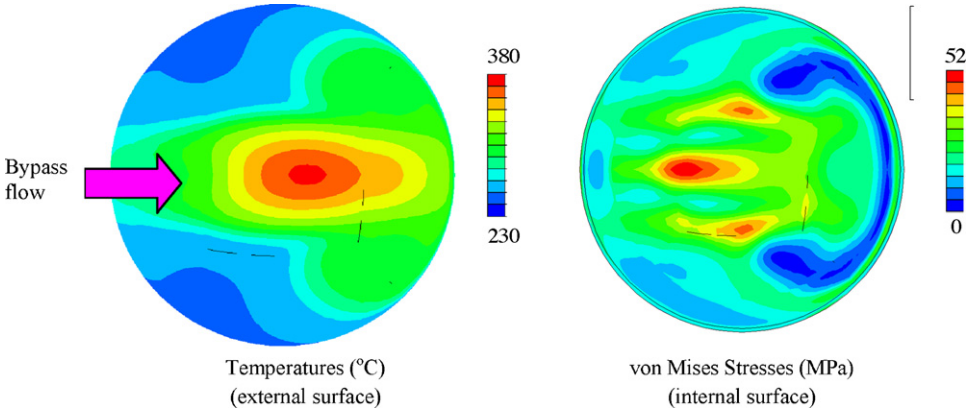

Fig. 9. Temperature and stress distributions over the window surfaces.

Coupled thermal-hydraulic and stress-analysis (Zucchini and Smith, 2003a) calculations indicate that jet impingement of cold (40 °C) D_2O from a ruptured LTE onto the hot (~400 °C) outer surface of the LLMC window would not lead to brittle fracture (Smith et al., 2004). The converse situation, of LBE leakage into the space between the LLMC and LTE hulls, has also been analyzed numerically, with beam heating (Smith and Shepel, 2005), and in terms of a full-scale leak test, with no beam heating (Samec, 2006). All indications are that the LBE would be contained, with no serious structural damage, nor blockage (through plastic deformation) or local boiling of the D_2O in the LTE cooling circuit. However, the peak temperature in the D_2O was measured in the test at 145 °C, only 15 °C below saturation under the prevailing circuit pressure (6 bar).

4.2.4. Validation studies

The flow visualization tests HYTAS have provided high-quality velocity measurements in a 1:1 MEGAPIE geometry at close to prototypic flow conditions ($Re \gg 60{,}000$ in HYTAS, $Re \gg 120{,}000$ in MEGAPIE). The flow is seen to be complex and time-dependent, with a critical value of the main/bypass flow rate (>15) necessary to stabilize conditions over the window. Full details are given in Section 7.1.4.

The 1:1 scale LBE tests carried out under the acronym KILOPIE-1 have produced heat transfer coefficients (HTC) measurements in the range 15,000–20,000 W/m^2 K, which are in accord with expectations from earlier tests using Hg, and with CFD predictions. It has not been possible to reproduce controlled heat fluxes from the window which are prototypic for MEGAPIE. Temperature measurements obtained in the LBE from the Heated Jet series of experiments (with no window heating) have provided information on the stability of the bypass jet flow, and indications of the fluctuations to be expected in MEGAPIE, More details of both test series are given in Section 7.1.4.

Through appropriate benchmarking exercises, principally the EU project ASCHLIM (Arien, 2003) and the MEGAPIE Benchmark (Smith et al., 2003), confidence in the CFD thermal-hydraulic predictions made for the MEGAPIE project has been established. In particular, the $k-\varepsilon$ turbulence model, including the use of a turbulent Prandtl number to model heat transfer via the Reynolds analogy, if used correctly, is able to reproduce the mean-flow conditions and heat transfer reliably (Smith, 2006). This study will be extended during the post-test analysis (PTA) phase of the MEGAPIE project, making use of data collected during the irradiation period (Section 9).

In summary, a balanced programme of numerical and experimental work has been conducted in regard to target thermal-hydraulics, aimed at first defining and then proving the robustness of the lower target design (see also Section 7). For the vital issue of window coolability, the picture which emerges from the available evidence is a consistent one. With adequate bypass flow maintained, a HTC in excess of 15,000 W/m^2 K has been predicted and measured over the heated part of the window, sufficient to keep the outer window temperature below the design value of 400 °C (370 °C/342 °C for a beam current of 1.74 mA/1.40 mA, respectively); the maximum inner surface temperature is about 35 °C lower than this. With inadequate or no bypass flow, a heat transfer coefficient (HTC) of 5000 W/m^2 K has been predicted and measured over the heated part of the window, sufficient to limit the maximum window temperature to 530 °C—hot, but a long way from compromising its structural integrity.

4.3. Assessment of the target containment materials

Experimental and numerical activities have been performed to assess the lifetime of the MEGAPIE target. This assessment has its focus on the lower liquid metal container (LLMC). However, the in-service behaviour of the lower target enclosure (LTE) and the inner target components were also evaluated.

4.3.1. Lower target enclosure

The LTE has been made of AlMg3, which was used for all safety hulls of the SINQ-solid targets. Two safety hulls were operated in the past without problems up to more than 10 A h proton charge which is well above the design value of 6 A h maximum proton charge.

4.3.2. Internal and upper containment structures

The internal (pumps and heat exchanger) and the upper containment structures, made of the austenitic steel AISI 316L, experience no or little radiation damage. As for the main/bypass flow guide tubes, central rod, fill and drain tubes, the calculated peak damage for a 6 A h proton charge is less than 5 dpa. In these irradiation conditions and the operation temperature range, the AISI 316L steel retain significant ductility, toughness and fatigue resistance (AAA, 2003). Further, it was shown that the low cycle fatigue life of 316L in LBE at 260 °C is little affected compared to the fatigue life in air (Kalkhof and Grosse, 2003). In addition, the corrosion rate at low oxygen content and in flowing LBE evaluated to be ca. 0.1 mm/year, should have very little impact on the mechanical resistance of these components. Therefore, and given the fact that the maximum stresses in the irradiated parts are relatively low (about 60–70 MPa), the 316L components up to the maximum envisaged proton dose does not represent a life-limiting factor for the MEGAPIE target.

4.3.3. Lower liquid metal container

The LLMC, and in particular the beam window, is the most critical component. The determination of its lifetime is very challenging, since many possible causes of damage are present and could act synergistically: corrosion/erosion by flowing LBE, irradiation embrittlement by energetic protons and neutrons, liquid metal embrittlement (LME)/liquid metal accelerated damage (LMAD), cyclic mechanical and thermal loading.

The corrosion/erosion of T91 in flowing LBE at 400 °C with a velocity of 1 m/s and low oxygen concentration was evaluated to be less than 130 μm/year. The corrosion rate of the beam window is probably lower than this value, because the nominal maximum operation temperature is lower than 400 °C. The reduction

in the window thickness corresponding to this corrosion rate (<60 μm in 5 months of operation) would not unacceptably weaken the component from a mechanical point of view. As such, corrosion/erosion does not represent a life-limiting factor for the target.

By contrast to corrosion/erosion, irradiation embrittlement in a spallation spectrum represents a critical issue with regards to the safe operation of the target. A main concern is the risk of sudden brittle failure of the window due to the irradiation-induced shift of the ductile to brittle transition temperature (DBTT) and the corresponding large decrease of the fracture toughness. Impact/small punch test data measured on T91 and other martensitic steel samples irradiated in SINQ, showed that the DBTT should remain below the minimum operating temperature (i.e. 230 °C) up to a proton charge of about 3.4 A h which corresponds to a damage of 8–9 dpa (Dai, 2004). The linear elastic fracture mechanics analysis made by Henry (2003), assuming the presence of a thumbnail crack on the inner surface of the window demonstrated a negligible brittle fracture risk, at least up to 8–9 dpa.

This analysis, however, does not take into account possible LME/LMAD effects. It has been shown that T91 is prone to LME if there is plastic deformation and intimate contact with the liquid metal (Van den Bosch et al., 2006; Aiello et al., 2004; Auger et al., 2004; Nicaise et al., 2001). Such conditions are not foreseen at the beginning of irradiation since the stresses in the MEGAPIE window were low and the material hardened substantially with irradiation. Moreover, during the pre-conditioning and the start up procedure wetting could be prevented by the presence of the native oxide layer. However, due to the production of hydrogen and other reducing spallation elements, it is expected that the oxygen content in the liquid metal can slowly decrease, at an unknown rate. Dissolution of the protective oxide layer may then occur, possibly leading to intergranular attack, as was for instance observed on T91 exposed for 4500 h to flowing Pb-Bi at 400 °C and low oxygen concentration (Aiello et al., 2004). Intergranular attack provides defects that can play the role of crack initiation sites which may propagate by cyclic loading in LBE leading to a strong reduction of the low cycle fatigue life (Vogt et al., 2005). However, fatigue crack formation and propagation is unlikely under MEGAPIE normal operating conditions due to the low stress amplitudes. The general trend is that the reduction in fatigue life in LBE compared to fatigue life in air disappears at low stress/strain values. Moreover, if a small crack were to form, due to the very low values of the stress intensity range ΔK to which the crack would be submitted, its growth rate would be very small ($<10^{-5}$ mm/cycle). Therefore, there is a very low probability that a crack of a few tenths of mm depth can be formed on the window inner surface. In addition, in the presence of such a surface defect, and taking into account the measured reduction in fracture toughness of irradiated T91 due to LBE (Dai et al., 2006) down to a value of 40 MPa $m^{1/2}$, the LEFM analysis presented in Henry (2003) still predicts that the brittle fracture risk is negligible. Based on the above discussion, a failure of the LLMC is considered unlikely within the projected service time of the target, under normal operating conditions.

5. Ancillary systems

The main MEGAPIE ancillary systems directly necessary for the target operation are the heat removal system (HRS), the cover gas system (CGS), the insulation gas system (IGS) and the fill and drain system (F&D). The basic functional requirements to the systems are described in the safety analysis report (Perret, 2002). For the technical layout we refer to (Corsini et al., 2003; Wagner et al., 2003a,b,c). The present description mainly focuses on the experience gained during the design and operational phases.

5.1. Heat removal system (HRS)

The HRS (Corsini et al., 2003) consists of two subsystems: an intermediate cooling loop with oil Diphyl THT as cooling medium (ICL), connected to the heat exchanger pins in the target, and second a back-cooling water loop (WCL). The ICL, operating between 160 and 230 °C, is primarily necessary to remove the about 0.6 MW of heat load deposited in the liquid lead–bismuth eutectic (LBE) by the proton beam. As a second function it must also be capable to manage a controlled hot-standby operation after beam trips or scheduled beam interruptions to prevent freezing of the target.

The general layout of the system proved to be sound. Oil as cooling medium turned out to be a reasonably good choice. The heat removal capacity of the system was rather over dimensioned. Oil degradation by radiolysis and pyrolysis was found to be much less than anticipated. The main drawback of using oil is the need for fire protection which was achieved by inertisation of the atmosphere in the target head enclosure chamber TKE and in the beam transport vault.

During the commissioning and test phase major and minor deficiencies have been discovered and repaired on site, demonstrating the importance of the quality assurance and component selection during the design and manufacturing phase.

5.2. Cover gas system (CGS)

The CGS (Wagner et al., 2003a) must handle the volatile radioactive and non-radioactive inventory of spallation products released from the LBE in the target. Handling of radioactive gases and volatiles imposes stringent requirements on safe and remote operation, on retention of radioactivity, like second containment and tightness, and on shielding.

The chosen design, in principle, proved sustainable; in practice, meeting the stringent requirements turned out to be rather complex and expensive. One lesson learned with the system was, that ‘leak-tightness’ for gases in the conventional definition is not the same as for radioactive gases: In spite of successful He leak tests according to specification a leak from the decay tank into the 2nd containment was detected by the very sensitive detector controlling the circulating gas. Although clearly detectable, the leak was sufficiently small such that the inventory could be released weekly by venting of the 2nd containment through the controlled exhaust system. A further lesson was to care for redundancy (if possible double) of vital sensors in such

a delicate system: one pressure transducer inside the enclosure controlling and recording the plenum gas pressure failed, most likely due to radiation damage, although qualified for radiation resistance up to a total Gamma-dose of 1 MGy. Switching to the remaining redundancy solved the problem at that time, but after that no redundancy remained.

A further critical issue is gas sampling, indispensable to control the inventory before venting. Reliable and quantitative gas sampling is a difficult action and can be a hazardous job which needs special precautions, not at least to prevent or minimize radioactive exposure of the executive personnel. Our initial concept using a glass phial and a needle to perforate the covering membrane turned out not to be a viable option. Rather, a qualified steel gas mouse with valve and flange connection was used.

5.3. Insulating gas system (IGS)

The IGS (Wagner et al., 2003b) fills the volume between the inner hot part of the target and the outer cold hull by an insulating gas. The concept envisaged was filling with He at a pressure of 0.5 bar, benefiting from lower activation on the expense of a higher heat loss compared to filling with Ar. During preheating the empty target it turned out that evacuation was necessary to prevent excessive heat loss. After the target was filled with liquid metal, during refilling the isolation volume with He we experienced that four out of seven electric heaters in the lower central target were damaged, probably caused by electric discharges. The loss of heaters did not hamper or inhibit further operation, but another draining and refilling with liquid metal would not have been possible any more.

One of the accident scenarios which needed to be safely handled was water ingress from a leaking safety hull into the insulating gas volume with the consequence of steam production and possible pressure built-up. This was accomplished by installing a 40 mm exhaust pipe combined with a rupture disk and a steam condenser vessel outside the insulation volume.

Designed as closed volume the pressure in the IGS was expected to remain constant during target operation, only reacting to temperature variations. Instead, starting with the first beam a continuous gas pressure increase of about 5 mbar/h was observed. Thorough analysis gave evidence that most likely oil from the HRS was leaking into the IGS volume and decomposed by radiolysis during beam operation. The gas produced further contained small amounts of (radioactive) cover gas, entering through a second (small) leak. The gas production urged a weekly venting of the IGS. The measures taken to cope with this problem were the installation of a 180 l decay vessel in the cooling plant and regular (weekly) venting into the exhaust system after a sufficient decay period and gas sampling.

The lessons learned: do not rely on closed volumes, expect radioactivity everywhere and provide devices to handle that (for the case).

5.4. Fill and drain system (F&D)

The initial baseline for the F&D system required draining of activated LBE from the target after the operation period. A detailed design for that was elaborated; however, the draining option was recognized to bear considerable risks, immediate ones for accessing the TKE and more general ones related to licensing. As well, it had required considerable extra expenditure in the technical realization: besides the standard equipment like heaters for the LBE vessel, the valves and the pipes combined with appropriate thermal insulation, the active draining option would have imposed the need of radiation shielding, second containment, radiation-hard components and remote operation, similar to the CGS.

Viewing these difficulties the decision was taken to abandon the initial concept in favour of only inactive draining and final freezing of the LBE in the target after completion of the irradiation experiment (Wagner et al., 2003c; Turroni, 2005). The experience showed that switching to only non-active draining (filling and freezing) was essential for the realization of the irradiation phase in time. The inherent final freezing imposes mechanical stressing of the hull and window material due to the well-known volume expansion of solidified LBE (Zucchini, 2002a, 2004; Zucchini et al., 2003, 2005; Agostini et al., 2004). Hence, post-irradiation alterations of the materials properties are not completely excluded. This drawback is handled by controlled slow freezing of the LBE in the lower target volume.

The finally realized concept is sound; the system is reasonably safe and easy to operate. The experience during commissioning recommends providing sufficient trace heaters and place controlling thermocouples at the coldest points to prevent clogging. The missing oxygen control did not impose a problem.

6. Beam monitoring and LBE leak detection

Systems which make sure that no liquid metal can leak out of the target are of utmost importance for the safety of the MEGAPIE experiment. In the case of breaking the integrity of the lower target enclosure in the SINQ, LBE would spill into the beam line and cause a major accident. While the impact to the environment could be kept within acceptable limits, the situation for the PSI SINQ installations would be very serious (Perret, 2002).

It has been considered that undesired accidents to the SINQ facility can be initiated by an improper intensity distribution of the incident proton beam or the continuation of irradiation of the target while a significant quantity of liquid metal leaked into the lower target enclosure (LTE). Therefore, rapid detection of deviating beam or containment conditions and, common to both, timely switching off of the proton beam is required (Thomsen, 2006a). The MEGAPIE target can withstand a non-scattered fraction of 17% of the nominal beam for an extended period of time. With a completely non-scattered beam the peak intensity rises by a factor of about 25, which can cause the failure of the LLMC and subsequently also of the LTE after 170 ms. With respect to leak detection the situation is not as critical. Conservative assessment yielded basic requirements for these safety systems:

- The proton beam has to be switched off within 100 ms if 10% of the protons by-pass Target E (corresponding to an increase in peak intensity by a factor of two).
- The proton beam has to be switched off within 1 s if (0.5)1 of LBE is collected inside the LTE (corresponding to a level of leaked liquid LBE where about 2 kW of beam power are deposited in this volume)

Beam safety devices newly installed to guarantee a correctly scattered beam at the Megapie target are the Transmission Monitor, the Slit KHNY30 and the VIMOS.

The footprint of the beam is determined by scattering of the protons in a so-called Target E. The three independent systems not only provide redundancy but are also truly diverse in that they monitor distinct effects caused by the correct passage of the beam through target E (Thomsen and Schmelzbach, 2006). The beam current is reduced by 30% after target E; this is checked by the current monitor (Duperrex and Müller, 2006). Non-scattered protons have a somewhat higher momentum than correctly scattered ones; they take a different path through the bending part of the beam line beneath the SINQ target (Rohrer, 2001). VIMOS monitors the glowing of a screen heated by the protons just in front of the spallation target; it looks for the issue in question most directly: a spot with high beam density is making the screen glow brighter than expected (Thomsen, 2005). Already during its commissioning phase VIMOS demonstrated its ability to detect potential harmful distortions in the beam footprint. Only very few times the beam safety devices interrupted the proton beam during MEGAPIE operation. These signals were the consequences of unexpected beam conditions. In addition, during the irradiation phase of MEGAPIE, the significantly increased neutron flux led to an accelerated degradation of the VIMOS camera, which was replaced successfully.

The LBE leak detectors installed in the MEGAPIE target were thermocouple and stripe sensors. The thermocouples were found out to be the only type of sensor, for which a record of reliable performance in the harsh radiation environment inside a SINQ spallation target existed; standard solid state targets are routinely equipped with such temperature sensors. In the MEGAPIE target six normal and three pre-heated thermocouples were installed at the bottom of the LTE. Leaking metal would be detected as a sharp transient in the monitored temperatures, in case of a sudden substantial leak; gradually developing leaks with very small quantities of LBE would be detected by checking the actual temperatures to expectation values derived from average beam conditions. Three stripe sensors consist of open capacitors, where the impedance, both Ohmic and for high frequency, is monitored. Because of limitations for the possible qualification test of such a device the stripe sensors were classified as ancillary equipment and not as the primary leak detectors (Thomsen, 2006b).

During the operation of the MEGAPIE target, except for the failure of one non-heated thermocouple, the temperature-based leak detector worked fine. Unexpected behaviour of the stripe sensors could be attributed to the effect of radiolysis products from a tiny leak of oil into the insulation gas volume around the liquid metal container inside the lower target enclosure. Even with the resulting strong and varying bias signal, a short circuit due to leaked LBE between the gold electrodes would have been detected.

However, other redundant information on the status of the LBE containment can be derived from a number of different measurements in the target, including cover gas and insulation gas pressure and the level of the LBE.

7. Testing before irradiation and overall target performance assessment

The individual components of the MEGAPIE target are directly linked with each other via electric, thermal and viscous boundary conditions acting on by orders of magnitude different time and length scales in a rather compact arrangement. However, a numerical simulation representing all transfer phenomena is far beyond the current numerical capabilities. Especially, due to the use of a heavy liquid metal as neutron spallation source and coolant, components as well as the associated monitoring/control instruments are required for which at present inadequate models or only insufficient descriptions are available. Indeed, with respect to systems making use of conventional components and for which availability and failure probabilities are well defined and described, the liquid metals dedicated components required several single-effect studies related to their basic functionality. Hence, for a unique installation like the MEGAPIE-target the overall performance analysis must be performed on two levels, i.e. a micro-scale analysis, by taking into account the single component tests and evolving from this a macro-scale analysis containing the component interaction which has been tested during the integral test.

The micro-scale analysis considers on a kinetic and rather local level each of the non-standard liquid metal components accounting for their reliability, availability, capability as well as monitoring and control aspects. Afterwards a macro-scale investigation by means of different system analysis codes was performed which incorporated experimental or numerical correlations found on the micro-scale. This rather standardized method considers the normal operation and transients occurring regularly due to the accelerator operation. Abnormal scenarios mainly associated with a failure of one or more active functional components were analyzed and the time frames on which counter-measures must be initiated to maintain the structural integrity have been defined.

7.1. Micro-scale analysis of the liquid metal components

7.1.1. Electro-magnetic pump system (EMPS)

The circulation of the lead–bismuth alloy within the target is generated by two independently controllable annular linear induction pumps (ALIPs) immersed in the upwards directed riser flow. While on the upper side located main pump is serving the main flow towards the heat exchangers (HX), the outlet bypass pump is guided through a ring shaped collector, which exits to the jet tube directed to the lower target shell. Both pumps, depicted schematically in Fig. 11(left), have been calculated

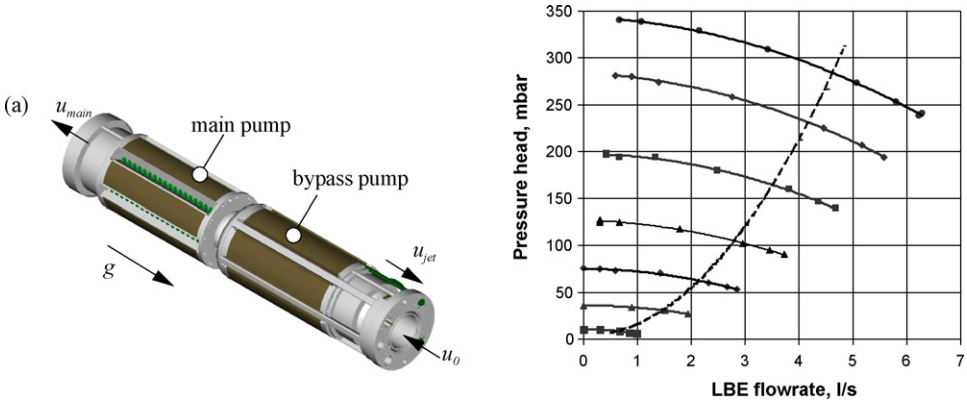

Fig. 11. (Left) Sketch of the arrangement of the EMPS; (right) pressure head—flow rate characteristics of the main flow electromagnetic pump for currents: (1) 33A; (2) 30A; (3) 25A; (4) 20A; (5) 15A; (6) 10A; (7) 5A; (8) hydraulic characteristic of the target main channel.

regarding their capabilities, the appearing thermal loads and their design margin (Freibergs and Platacis, 2002, 2003; Ivanov et al., 2006; Stieglitz, 2003; Stieglitz and Zeininger, 2005). The design requirements in terms of flow rate and attainable pressure head are exceeded for the pumps by 20–30% and, which was confirmed by the experimental activities (Dementjev et al., 2003, 2005) (Fig. 11).

7.1.2. Liquid metal flow meters

The flow rate measurement is recorded for each stream by an electro-magnetic frequency flow meter (EMFM). The measurement principle is that the motion of an electrically conducting fluid within an imposed field B produces an induced field B' being linearly proportional to the flow rate. The EMFM signal is directly electrical, inertialess, continuous and no transducer is required; moreover, no electrical connections to or inside the flow channel are necessary. Despite this attractive feature, tests conducted on the EMFM and Jekabsons (2006a,b) showed results of only qualitative nature (Freibergs and Platacis, 2006; Dementjev et al., 2005, 2006). Buchenau et al. (2006) and Jekabsons (2006a,b) analyzed the EMFM in detail recently and were able to identify the potential source of measurement errors and countermeasures, which could not be embedded before the MEGAPIE-start up. However, based on the tests performed the existence of a certain flow rate can be assumed by considering the magnitude of the electric power supplied to the pumps and the temperature readings on discrete positions (Ivanov and Dementjev, 2006). Since, especially the pressure flow-rate distribution as a function of the supplied electric power to the pumps has been calculated and experimentally measured within a threshold of ±15%, this reading with the supplementary calculation can be used to establish the required flow rate combination between main and bypass flow in order to ensure a sufficient beam window cooling (Ivanov et al., 2006).

7.1.3. Liquid metal heat exchanger

The heat released in the LBE by the proton beam is transferred through a secondary oil system via twelve equally circumferential spaced pin heat exchangers, in which in each the oil is pumped through a cylindrical tube u-turned and guided spirally upwards to a collector. The heat transfer in each pin from the helically flowing Diphyl-THT® oil to the counter-current flowing LBE occurs in an annular small gap of 2 mm width along a height of about 1.2 m. Complementary to an analytical assessment using different heat transfer correlations, an experimental prototypical pin was tested (Agostini and Baicchi, 2002) and a fully 3D computational fluid dynamic calculation of the experiment was performed by Buono et al. (2001, 2002). The maximum discrepancies between experiment and 3D calculation were about 3.5%. The deviations between analytical descriptions and numerical solutions were about ±25% and depending on the different correlations available for LBE and oil. The heat transfer within the heat exchanger is mainly determined by the oil which has two orders of magnitude lower heat transfer coefficient with respect to the liquid metal. The global heat transfer has been validated with a geometrically scaled 1:1 experimental test (Meloni et al., 2006). The experimental results, as reported in Table 2 were analyzed by RELAP5 code in its standard version (inclusive of the Dittus–Boelter correlation) and in a new modified version. The modified version evaluates the oil side by the Gnielinski correlation having the Fanning coefficient evaluated according to it.

The experiment demonstrated that the CFD and the modified RELAP5 calculations describe carefully the heat exchange yielding a conservative assessment in terms of the heat transfer capability. The safety margin in terms of the heat transfer is more than a factor of two according to the technical capabilities of the secondary coolant side, so that a reduced performance of this loop does not lead to a failure of the target. Also the temperature limit of the oil with a boiling point of 380 °C is by more than 150 °C not reached.

Based on the CFD data a thermal stress analysis and fatigue calculations were performed using finite element method (FEM) and the RCC-MX method (Cadiou, 2004). Both methods evaluating the structural integrity showed safety margins of a factor of two.

7.1.4. Thermal-hydraulics experiments of the lower target shell

A unique feature of the MEGAPIE target represents the lower target shell, where the turbulent LBE-flow acts both as coolant and spallation target material. The challenging task to

Table 2
Discrepancies between experiments on a prototypical pin and corresponding RELAP5 calculations

	E1			E2		
	Experimental	Unmodified RELAP	Modified RELAP	Experimental	Unmodified RELAP	Modified RELAP
Power (W)		27,430			21,590	
Oil inlet T (K)		410.15			409.35	
Oil outlet T (K)	436.65	436.90	436.90	430.25	430.79	430.8
LBE inlet T (K)	579.05	592.31	579.94	537.25	550.82	535.33
LBE outlet T (K)	455.95	473.19	461.38	445.85	462.64	447.71
H global (W/(m^2 K))	1790.04	1407.2	1596.68	1831.14	1368.57	1714.52
Percent error		21.4%	10.8%		25.3%	6.4%

design this lower target region without exceeding the material acceptable temperature, stress and irradiation limits demanded extensive CFD studies as already described in Section 4. These studies have shown that a sufficient cooling of the beam window in the MEGAPIE set-up is only achieved if the flow is appropriately conditioned (Tak and Cheng, 2001; Roubin, 2001, 2002, 2003a,b, 2004). This is realized in a cylindrically shaped geometry, in which the main flow is guided in an annular gap downwards and then u-turned close to a hemispherical shell into a slanted riser tube. In order avoid stagnating fluid domains leading to unacceptably high window temperatures a jet flow is injected in direction of the lower shell. The absence of detailed turbulence models describing the heat transfer in liquid metals adequately required an extensive experimental program supporting the CFD data. Because out-of-pile heat production scenario as in MEGAPIE is hardly feasible three experiments were defined clarifying the following issues:

(a) The isothermal water experiment HYTAS (hydraulic behaviour in spallation target systems) (Lefhalm et al., 2005) to measure the flow pattern and the velocity distribution and to compare them to numerical computations.
(b) The heated jet experiments (Daubner et al., 2004, 2005), where a heated jet is injected into the cold main flow to investigate the thermal mixing in the lower shell. Since the temperature is acting as a passive scalar in such a set-up, besides the thermal energy exchange in the lower shell also HYTAS data can be evaluated in a LBE configuration.
(c) The KILOPIE (kilowatt pilot experiment) experiment, where the heat transfer from the beam window is evaluated by means of heat emitting temperature-sensing surfaces (HETSS) simulating the heat release of the proton beam in the MEGAPIE beam window (Patorski et al., 2000, 2004).

Even if, the volumetric heat generation cannot be simulated in out-of-pile experiments, it can be computed quite reliably also for low Prandtl number fluids once the flow pattern and velocity distribution is verified by the previous described experiments (Smith, 2002).

In Fig. 12 the HYTAS set-up as well as flow visualizations in the lower target shell obtained by laser light sheets (LLS) are shown for a main (Q_{main}) to bypass (Q_{jet}) flow rate ratio of $Q_{main}/Q_{jet} = 15$ as it may appear in MEGAPIE. The illuminated regions in the LLS exhibit the streamlines of flow. The flow pattern detected is rather complex and composed of different single effects interacting with each other. Fig. 12b shows a large-scale recirculation zone is formed in the riser tube for $\phi = 0^\circ$. The combined momentum of jet and main flow leads to a strong deflection of the main part of the fluid flow towards the riser tube side opposite the nozzle exit. Here, an area with a high velocity jet is observed. At the boundary between the recirculation domain and high velocity region a set of counter-rotating vortices is visible, see Fig. 12c. The introduction of the jet extinguishes the small recirculation area close to the inner side of the riser tube at $\phi = 180^\circ$ totally. Due to the jet flow the stagnation point is shifted to the opposite side of the nozzle. For $Q_{main}/Q_{jet} = 15$ it is approximately located at $r = 55$ mm, $\phi = 180^\circ$. A closer view on the light-sheet shows a peculiar feature of this flow rate combination with respect to the MEGAPIE application. The streamline in Fig. 12d shows that the jet hits the wall close to the centre line at about $r \approx 20$ mm, $\phi = 0^\circ$ and then detaches from the wall. However, in this part of the window the highest surface heat flux appears and thus requires the best heat transfer characteristics. A part of the jet re-hits the hemispherical shell again for $r \approx 30$ mm, $\phi = 180^\circ$.

A parametric study regarding the flow rate rations exhibited that only for $Q_{main}/Q_{jet} \leq 12.5$ the jet covers sufficiently the whole lower shell in both planes $\phi = 0^\circ$–180° and $\phi = 90^\circ$–270°.

For all MEGAPIE relevant Reynolds numbers the flow is strongly time dependent and the fluctuation intensities are of the order of the mean velocity. A comparison with the CFD data confirmed the established flow pattern in dependence of the flow rate ratio, however, the quantitative values differed considerably. The HYTAS experiments also exhibited that the MEGAPIE design is sensitive to marginal deviations of symmetry leading to the induction of secondary flows and to upstream history effects. However, their magnitude of 10–15% does not affect the general heat transfer capability beyond this range.

The heated jet experimental series fulfilled two aims. On the one hand it offered the capability to use temperature readings as a tracer to conclude on the velocity distribution in order to verify the HYTAS campaigns and on the other hand to investigate the thermal mixing of the flow in the shell region and downstream in the riser tube, which allows to determine the flow rate ratios for which the flow covers the shell, their stability and the temperature distribution in the riser tube. This thermal measurement is important since almost all power is generated as volumetric

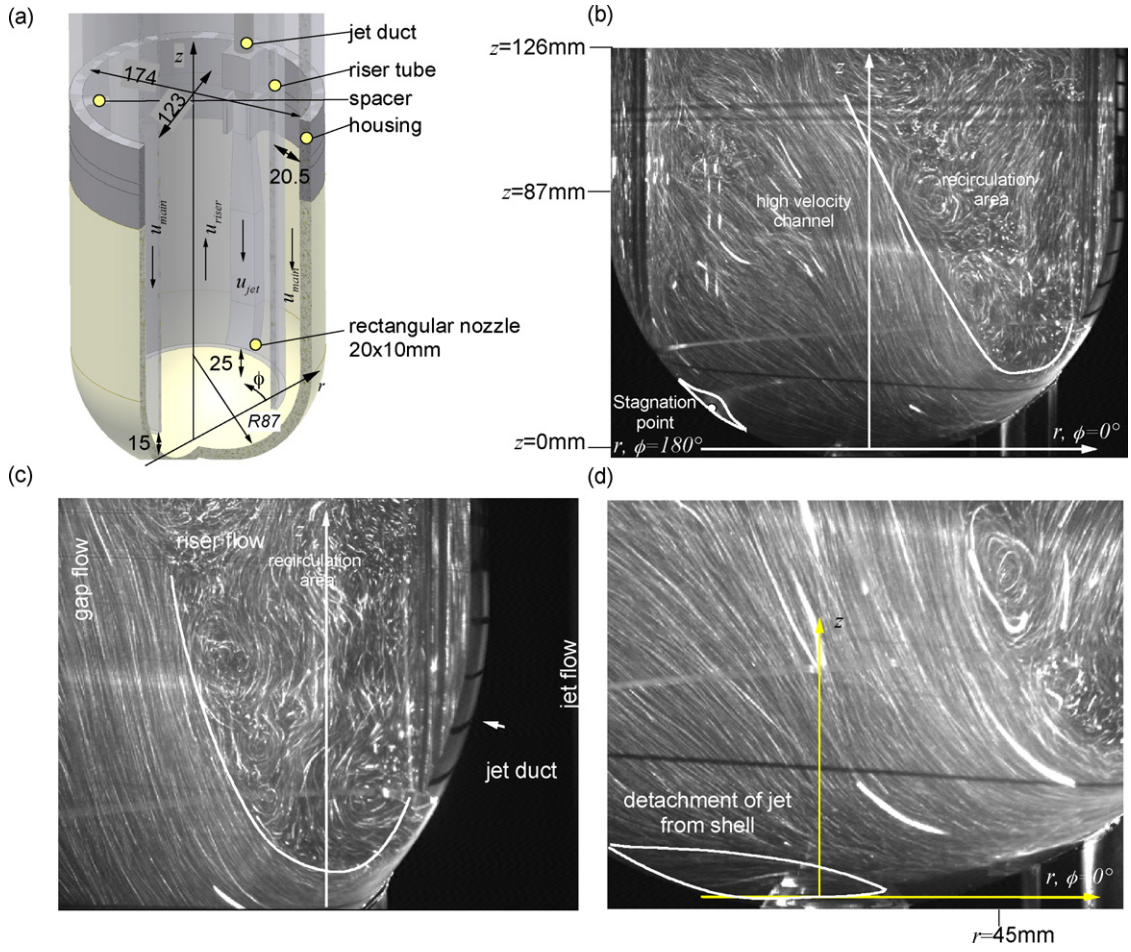

Fig. 12. (a) Geometric dimensions of the HYTAS Set-up (Lefhalm et al., 2005) and introduced coordinate system. (b)–(d) LLS-Photographs of the fluid flow in the MEGAPIE-HYTAS water experiment for a slanted riser tube with a jet flow $Q_{main}/Q_{jet} = 15$ for $\phi = 0°$–$180°$, Remain = 5.9.104. (b) Lower shell with different flow regions; (c) close view on the jet flow exiting the nozzle and the adjacent riser flow; (d) close-up of the streamlines at the shells center.

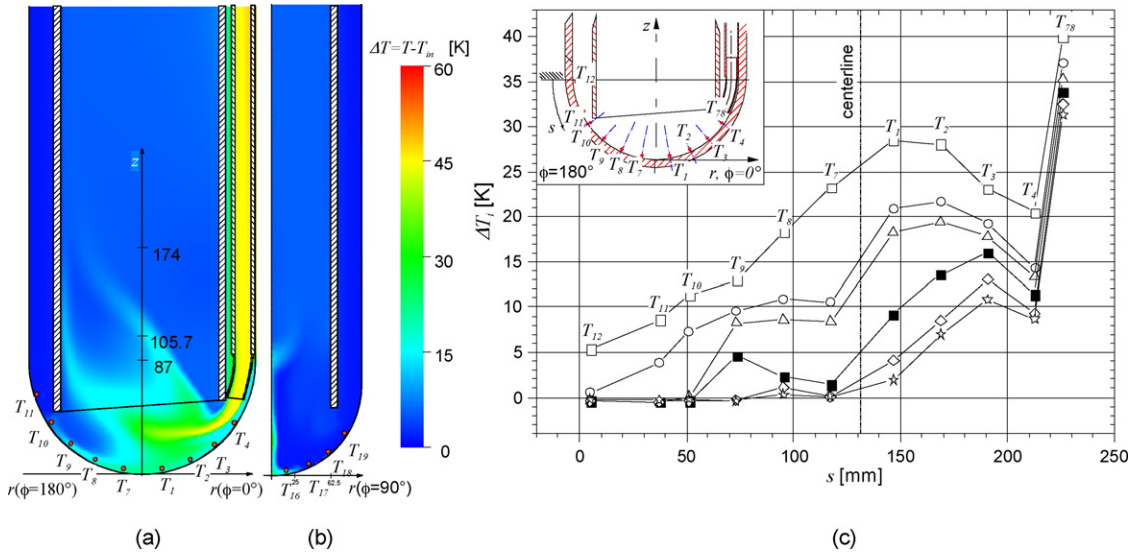

Fig. 13. Calculated temperature difference contours for $Q_{main}/Q_{jet} = 15$ in the (a) r–z-plane ($\phi = 0°$–$180°$) and (b) r–z-sector ($\phi = 90°$). (c) Measured temperature distribution as a function of the geometry adapted coordinate s in the plane $\phi = 0°$–$180°$ for different flow rate ration Q_{main}/Q_{jet}. (□) $Q_{main}/Q_{jet} = 7.5$, (◯) $Q_{main}/Q_{jet} = 10$, (△) $Q_{main}/Q_{jet} = 12.5$, (■) $Q_{main}/Q_{jet} = 15$, (◊) $Q_{main}/Q_{jet} = 17.5$ and (☆) $Q_{main}/Q_{jet} = 20$.

heating and an insufficient mixing could lead to a distortion of the riser by differential thermal elongation with all the accompanying consequences. Fig. 13 shows computed and measured temperature distributions along the lower shell. Fig. 13a and b shows that the fluid mixes nearly complete in short distances downstream the riser tube, while Fig. 13c exhibits that only for flow rate ratios of $Q_{main}/Q_{jet} \leq 12.5$ the jet covers the whole lower shell confirming the HYTAS data. The minimum flow rate required to transfer the heat was found to be about 60% of the main pumps capacity at nominal power. All flow pattern detected were time dependent, but the temperature fluctuations recorded were all larger than 1Hz not leading to a fatigue of the beam window by thermal cycling (Daubner et al., 2005).

The remaining issue to be clarified by the KILOPIE series was the determination of heat transfer coefficient at the fluid wall interface of the beam window facing the proton beam. Therefore, the HETSS technique was developed, with which both the heat flux can be simulated and the temperature distribution can be evaluated. The experiments, carried out both at PSI and at the KALLA loop at the Forschungszentrum Karlsruhe, confirmed that a sufficient heat transfer coefficient is obtained for almost the same flow rates as detected in the heated jet series.

The tests described above were on prototypic components. However, in the case of the EMP and of the flow-meters tests have been carried out also on the real components (Dementjev et al., 2005).

7.2. Macro-scale analysis of the whole target

7.2.1. Systems integration

An important milestone before the target irradiation in SINQ was the MEGAPIE target integral test (MIT). The main objectives of the MIT were: to integrate the liquid metal target and the ancillary system under a single MEGAPIE Control Module; to test and to verify the function of the ancillary systems, the EMPS and the heat exchanger; to set the control parameters and conditions for the irradiation experiment in SINQ and to train the operators. In Fig. 14 the MEGAPIE integral test stand (MITS) is shown.

The thermal-hydraulics performances of the target and the heat removal system have been assessed in scaled conditions simulating the operation in SINQ. The proton beam was simulated with a 165 kW electrical heater. The standard (700 kW) water heat exchanger was replaced by a low-power one (240 kW). Water and oil temperatures and flow rates in the loops were adjusted and maintained in accordance with preliminary calculated scaled conditions.

The previously described micro-scale analysis formed the basis of the macro-scale analysis describing the component interaction evaluated at the MITS. The LBE system is connected to the general heat removal system (HRS) and is thus significantly influenced by it. However, the HRS consists of components commercially available (pumps, valves, flow meters, piping and geometries) operating with standard media (oil and water) so that in this context a detailed micro-scale study was not performed. Each of these components was described in its performance and characteristics with the data delivered by the manufacturer or determined in experimental campaigns.

The HRS, as described in Section 5, is designed as a double loop and is connected to the primary LBE loop containing the target, the pumps, the lower target shell and a 12 pin oil/LBE heat exchanger. The oil operated intermediate cooling loop (ICL) consisting of pump, a three-way valve and an oil/water heat exchanger (IHX) is connected to the water cooling loop (WCL), which transfers itself the thermal energy to the coolant plant located in the building.

The macro-scale analysis on the energetic level was performed with the two system analysis codes RELAP5 (Petrazzini and Alemberti, 2002; Leung, 2004) and ATHLET (Chen and Cheng, 2005). The functional diagram depicted in Fig. 15 was developed and different scenarios were calculated.

Even if SINQ is a continuous neutron source, the proton beam power undergoes several transients a day which are associated with the operation of the accelerator. Typical transients are beam trips (instantaneous beam shut down and automatic restart with a 20 s ramp to full power), beam interrupts (the beam is shut down without automatic restart) and beam restart. The system analysis of all transients cases (Chen and Cheng, 2005; Leung,

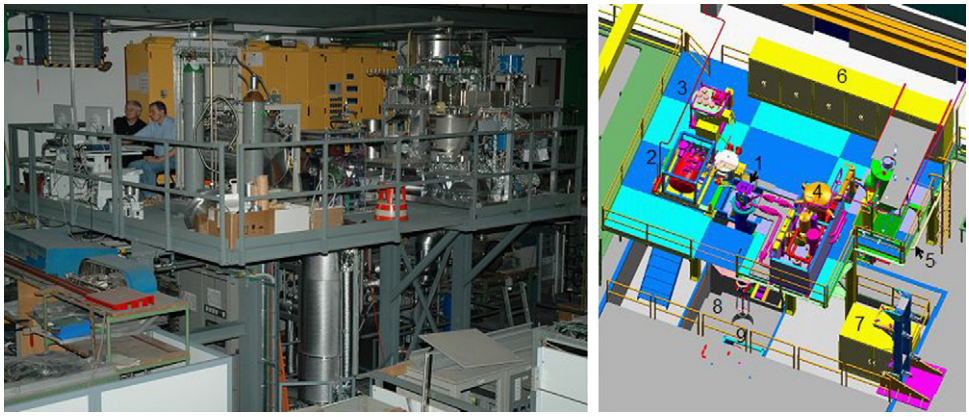

Fig. 14. MITS, general view and arrangement of subsystems: the elevated platform bears the target head (pos. 1) with its connections the PbBi tank (2), the cover gas system (3) and the heat removal system (HRS, pos. 4) in the same geometric arrangement as in the SINQ. The control system cabinets (6) are in the back of the platform. On the ground floor and in the basement intermediate water-cooling loop and electromagnetic pumps (EMP) power sources are situated.

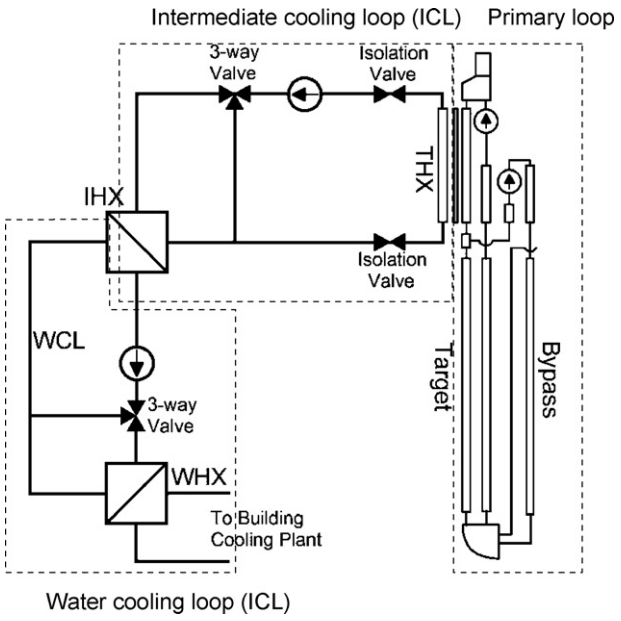

Fig. 15. Functional diagram of the MEGAPIE heat removal system (HRS).

2004) showed that during the beam trip an adjustment of the three-way valves in the ICL and WCL is needed. On the other hand, for a beam interruption, the electrical heater, installed at the central rod, enables to reach within 118 s about 220 °C as the lowest temperature, which is considerably above the melting point of LBE.

Besides the normal operation, transient scenarios which are initialized by the failure(s) of individual active components in the HRS were analyzed. According to this analysis the associated countermeasures are specified and the events were classified into three main groups:

- The target can be operated with marginal loss of performance.
- The target can be restricted operated for a certain time
- The target must be immediately shut down.

Since the component interaction is treated on an energetic level, an excess of the maximum tolerable temperatures or stresses may occur locally, which depends on the accidental event and induce additional failures. For these cases temperature/stress margins as well as time thresholds were defined, for which no local excess can be expected. For instance regarding the time scale a failure of an active component like a pump (loss of flow accident) should require counter-measures in terms of the time periods to react, which should be considerably larger than the detection time by the programmable logic controller (PLC) installed in the MEGAPIE target (1second) plus the active operation of the counter-measure. MEGAPIE specific incidents and the related consequences have been assessed:

- Failure of the main electromagnetic pump (EMP). If the proton beam remains on, buoyant convection leads immediately to a remaining flow rate of 20% of the nominal one. The temperatures at the beam window and in the riser tube increase by 100 °C within 120 s. This time scale allows sufficient margin for safe shutdown.
- Pump trip in the ICL. About 5 min after the trip the LBE temperature rises up to 500 °C. Then the oil in the ICL starts boiling. Also this event allows sufficient margin for a safe shut down.
- Pump trip in the WCL. It has been calculated that 90 s after the event boiling of the water can occur, thus allowing sufficient margin for a safe shutdown.
- Loss of one or more heat sinks while the proton beam remains on. In this case three critical temperatures appear, the limiting LBE temperature ($T_{LBE} = 550$ °C), the boiling temperatures of the oil ($T_{b,oil} = 341$ °C) and water ($T_{H_2O} = 140$ °C) at the individual pressure levels. Such an incident occurring at nominal power level leads first to a boiling of the oil after about three minutes.
- Local LBE freezing is potentially possible in absence of the proton beam and unregulated cooling. However, the thermal inertia and heat capacity of the MEGAPIE design is so large that even in case of using the full cooling capability of the ICL and WCL a potential solidification could be conservatively assessed earliest after 230 s, which is considerably larger than the operational time of both PLC and all active components.
- Failure of the three-way-valves (TWV) (e.g. blockage or an electric supply defect). In case of the TWV defect in the WCL with a pass through of only 30% of the nominal flow rate MEGAPIE can still operate without any changes. More problematic is the TWV in the ICL, requiring at least a pass through of 60%, because the thermo-physical properties drastically change close to the boiling point, increasing the uncertainty threshold.

The analysis of all considered time dependent modes that can potentially occur (both normal operation transients and abnormal or accidental events) led to time frames easily to be detected by a PLC and/or an operator. None of these scenarios is at the edge of the inertia of the participating individual components, which documents the robust thermo-mechanical design of MEGAPIE.

The system analysis was confirmed by the MITS out-of pile experiments (Leung, 2005, 2006). All individual tests performed at the MITS showed deviations in the range of ±10% from the predictions of the system analysis codes.

The overall performance of the MEGAPIE target is assessed with the main focus on the LBE components unique to this installation. This refers both to the micro-scale analysis conducted on a rather local detailed study and a macro-scale analysis treated on an energetic level describing the component interaction of the LBE system with the subsequently arranged oil and water loops for different prescribed normal and abnormal operation transients.

Related to the micro-scale analysis, all major LBE components (i.e. the pumps, the pin heat exchangers and the lower target shell) show safety margins of at least 25% with respect to their maximum capability. A set of out-of-pile experiments for each component conducted at prototypical dimensions and MEGAPIE relevant temperatures and flow rates, which all were

supported by CFD and stress analysis codes demonstrated and proofed this threshold. Only the electro-magnetic frequency flow meter showed an unacceptable performance for several reasons very recently explained. However, a reliable operation can be ensured, with acceptable accuracy, through the monitoring of the EMPS electric power supply.

The computational analysis of all pre-defined transient operation scenarios occurring during normal operation and transients, revealed acceptably large time scales for the detection and the initiation of countermeasures to operate the target safely. The simulations were performed using different codes and showed in comparison with a benchmark experiment conducted with the MEGAPIE-module except for the lower target shell a reasonable agreement. Despite the fact that several single-effect studies exhibited discrepancies to the corresponding experimental tests none of the found disagreements added up to a large uncertainty factor, which demonstrates the robust and reliable design of the MEGAPIE-target.

8. Safety and licensing of the MEGAPIE experiment

8.1. The framework

Design, construction and operation of the MEGAPIE experiment has to comply with Swiss Law and Regulations.

The legal bodies involved in the licensing process were: The Swiss Federal Office of Public Health (BAG) is the responsible authority for all non-nuclear installations at PSI. The Swiss Federal Nuclear Safety Inspectorate (HSK) is the competent authority for activities in the Interim Storage of the Swiss Nuclear Power Plant (ZWILAG) and the PSI Hotlab, where dismantling, investigations and waste conditioning are planned. HSK is also competent for the licensing of transport containers. The National Cooperative for the Disposal of Radioactive Waste (NAGRA) evaluates specifications for the final waste disposal, which are then approved by HSK.

The original license of the SINQ operation stipulates that an additional license is needed, if targets will be used having a significantly higher hazard potential than those described and qualified during the SINQ licensing process. Since only solid zircaloy and lead targets were qualified, a liquid lead–bismuth eutectic (LBE) target requires additional licensing due to its high polonium inventory.

PSI has been dismissed from the duties derived from the emergency ordinance in case of accidents in nuclear installations, which requires that the dose of the radioactive fall-out for the public is markedly below 1 mSv for accidents with a probability larger than 10^{-6} year^{-1}. The MEGAPIE experiment therefore had to prove that this dose limit can be kept. In addition, emission limits had to be respected for normal operation and incidents. The air-born emissions are referenced to the accumulated dose at the closest habitation calculated with the code ESS41. Theses limits have been set for SINQ at 75 μSv for the annual accumulated dose, 18.75 μSv for the 3-month accumulated dose and 5 μSv for the short-term dose per event.

8.2. Preliminary safety assessment report

The preliminary safety assessment report (PSAR) (Perret, 2002), submitted to BAG, constitutes the basis of an application by PSI for a permit for construction of the MEGAPIE target system and its experimental operation in the SINQ facility. It deals with the following topics:

- Design, construction and operation of the experimental target system with a liquid lead–bismuth eutectic, which is to be installed in the SINQ spallation neutron source of PSI, quality management and functional tests of this target system prior to installation.
- Measures to cope with credible accidents in which radioactivity may be involved.
- Radiation protection measures, especially those taken to minimize personnel doses and collective doses and to limit radioactive emissions.
- Decommissioning, conditioning and disposal of the radioactive waste.

The PSAR demonstrates that compliance with the legal regulations about radiation protection, the guidelines of regulatory authorities, and the rules of PSI in-plant radiation protection is ensured in the design.

BAG granted the permit for the execution of the experiment imposing 5 milestones to be achieved and several prerequisites to be fulfilled.

The milestones, which had to be achieved, were:

- Inactive operation of the heat removal system.
- Inactive operation of the cover gas system.
- Inactive operation of the target system.
- Dismantling and disposal of the target.
- Active operation of the target system in SINQ.

Each of the milestones was cleared by an inspection of the existing equipment and of the corresponding Quality Assurance-documentation.

Based on the PSAR, BAG requested additional details on 52 topics to be submitted prior to the start of irradiation. These topics comprised details on testing, radioactive inventory and radioprotection as well as additional data on release characteristics of volatile spallation products, in particular Po. Draining of the active LBE was a concern, which was eliminated by the decision to freeze the LBE in the target at the end of the experiment. Organisational aspects and quality management issue were further topics which needed more detailed descriptions. Finally, two key issues were raised, which needed additional efforts and investments to comply with: fire protection and the definition of a reference accident case.

The use of the diathermic oil Diphyl THT® as secondary coolant raised concerns about fire protection/prevention in the target head enclosure (TKE). This had not been an issue before at SINQ, where only heavy water had been used as coolant. Although risks could be almost ruled out during normal operation, since the flame point of the oil is close to the operating

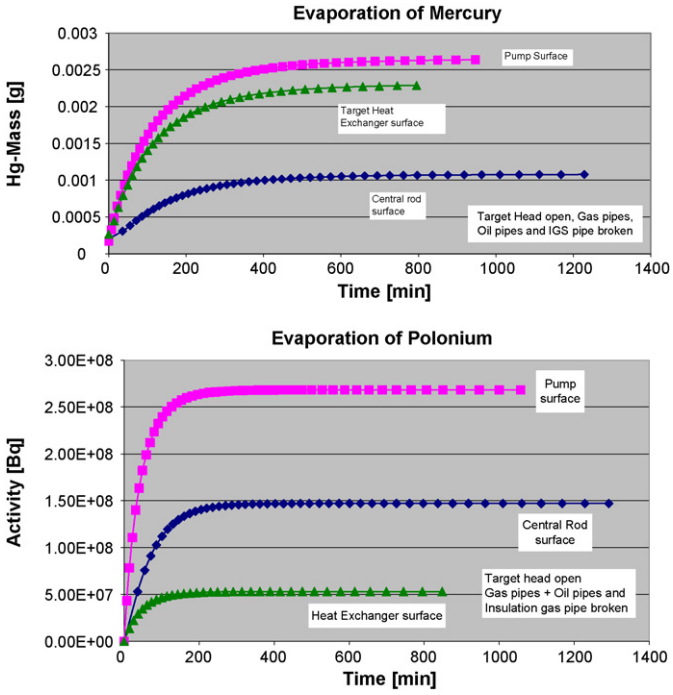

Fig. 16. Release curves for Hg (left) and Po (right).

temperature, this value may be exceeded during hot standby and in the case of accidents. In order to overcome this flaw, a system injecting nitrogen into the TKE and the beam transport vault (STK) has been installed to maintain the oxygen level below 13%. Tests have shown that the flammability of the oil can be successfully suppressed at that level up to 230 °C.

8.3. The reference accident case

In the PSAR, a number of possible accidents and their impact on the dose to the public have been analyzed. It was demonstrated that the limits imposed by the laws could be respected with the measures taken. However, the authorities decided to define an all-encompassing reference accident case, which has to be mastered to get the irradiation permit. The accident scenario is as follows:

- The target boundaries are breached due to an internal or external event and the LBE is spread into the beam transport vault. The target head is damaged and a communication is created between the beam transport vault and the TKE.
- The oil loop is damaged oil spills within the TKE and down the target and catches fire.
- The outer barrier is breached by rupture of penetrating pipes or ventilation ducts.

Analysis of the scenario identified three source terms for the release of volatiles:

- The expansion volume of the target containing the noble gases and a small fraction of other volatiles as mercury and polonium.
- The LBE spill in the transport vault.
- A thin film of LBE adhering on the wetted surfaces of the target (0.4% of the total mass).

Due to the slow cooling of the target by the ambient air, the release of the volatiles from the film became the dominating source term. Fig. 16 shows the release over time from the target film.

Calculations of the impact to the public showed that only the internally initiated event, in which the outer barrier stays intact, could be managed with the planned upgrade of the ventilation system. For externally initiated events, such as earthquakes, additional upgrading was required, which consisted of

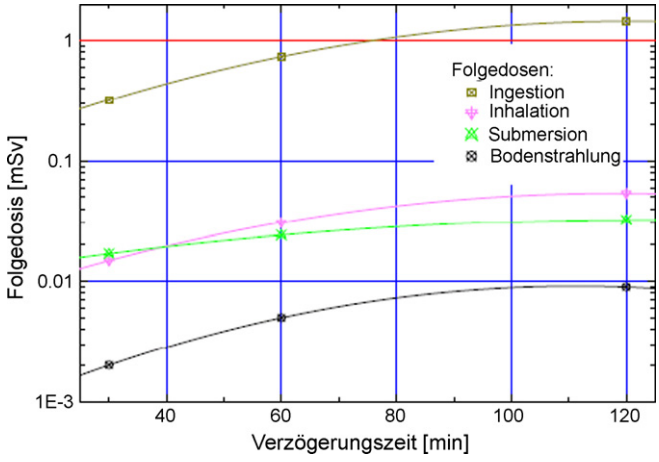

Fig. 17. Dose to the public as a function of delay in start of the autonomous filter unit.

- Equipping all ventilation ducts penetrating the barrier with earthquake resistant dampers, which close at a given seismic event.
- Strengthening the TKE outlet duct to resist the seismic event and connecting it to an autonomous, earthquake-proven filter unit. The filter unit automatically starts after the event and extracts the contaminated air. In addition, a mobile filter unit was kept as backup.

Fig. 17 shows the evolution of the maximum dose to the public in the case of such an event and the effect of the delayed start of the filter unit. It shows, that due to these measures, the dose can be kept below the stated limit of 1 mSv. Only after more than 60 min delay in starting the filter unit, the total dose would exceed the limit. With the ingestion dose not being relevant in this case, the grace time for starting the filter unit extends to days, which was considered acceptable.

In conclusion, having cleared all open issues, the final permit for start of the irradiation was received on 11 August 2006. The main goal to demonstrate licensibility of such experiments has been achieved. Although safety in design and operation is a prerequisite, the behaviour during severe accidents and the corresponding dose to the public dominates the licensing process. As expected, the control of volatiles is a key issue.

9. Irradiation and post irradiation phases

9.1. Irradiation phase

After a systematic check of the functionality of the target system and of the ancillary components, the target was preheated within 1 day up to 140 °C and filled within one hour with 926 kg of LBE. Off-beam operation in the hot standby mode (i.e. at an LBE temperature of 230 °C) to recheck proper functioning of the system and compare it with the integral test behaviour has been performed. Hot standby operation was used also to verify pump flow direction and pump performance, recalibrate the flow meters and the flow measuring system based on heat balance, determine the heat losses to the second enclosure and simulate the isolation case (loss of heat sink). The control and safety systems have been checked and operation was tested in manned and unmanned mode. The final upgrade of the ventilation system and the installation of the inertisation system were accomplished followed by a final inspection by the authorities. The TKE and beam transport vault were closed and an oxygen level <12% was established.

According to the start-up plan of irradiation, the proton current level, in a first phase, was limited to 40 μA over a period of ~1.5 h, yielding a total charge of 60 μA h. This phase served to measure the first neutrons on the instruments at the beam-lines and perform an end-to-end test of the beam interlock triggered by the slit system KHNY30. In addition, a check of the response of some target systems, like the LBE leak detectors and the neutron flux meters in the central rod, a first mapping of the dose rate distribution in the TKE and delayed neutron measurements were made. The beam power of 29 kW had only a very small effect on the thermal balance in the target. Since all systems performed as expected, phase 1 was concluded successfully.

In a second phase, the beam current was ramped in 50 μA-steps to 250 μA and was kept at that level for about 2 h. With 100 kW thermal power, the heat input corresponded to almost that provided by the heaters at MITS. A corresponding temperature rise was observed in the target and the heat removal system started to operate. The temperature control could well be followed during short intermittent beam stops. After an accumulated charge of about 800 μA h, the beam was stopped and fresh gas samples of the cover gas were extracted. In addition, a second set of γ- and n-dosimeters was retrieved from the TKE. Since the systems performed according to expectations, it was decided to ramp the beam up to full power.

In the third phase, the beam current was ramped in 100–150 μA-steps up to 0.9 mA within a period of 4 h. A further increase up to almost 1.2 mA triggered a large amount of beam trips caused by beam instability. This was a first severe challenge for the target, which was mastered perfectly. Total beam operation in this phase lasted about 9 h. During this period mea-

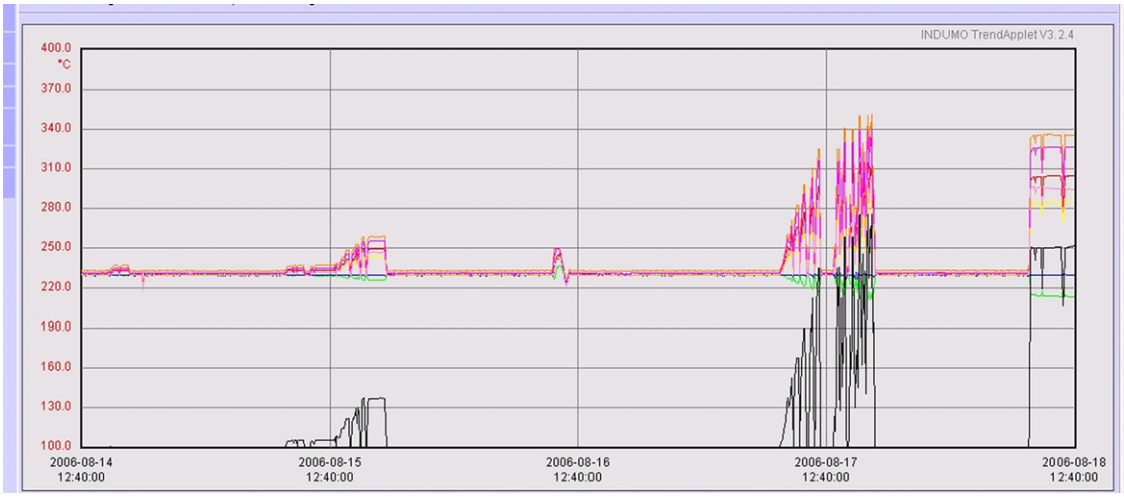

Fig. 18. Beam power (black, arbitrary units) and temperatures in the target during the start-up phase.

surements of the neutron flux meters in the central rod and of the VIMOS beam monitoring system were made. The LBE leak detectors were now fully heated by the beam and their margins could be adapted. Radiation mapping around the SINQ target block and in the neutron guide hall was performed. In this period a charge of 2.7 mA h was accumulated. Since the target operation was as expected, it was decided to continue normal operation, but limit the beam current at 1 mA in order to assure a beam as stable as possible. Fig. 18 shows the evolution of the beam on SINQ during the three phases and the corresponding temperature response within the target.

In a next phase the target has been operate at a 1.25 mA peak current for several days and finally the peak current was raised to maximum by maintaining stable beam operation.

9.2. Post irradiation analysis plan

A comprehensive analysis of the operation has started as part of the DEMETRA Domain of the EUROTRANS IP of the European 6th Framework Program (Fazio et al., 2005) with the aim to interpret the collected data during operation and dedicated tests and to compare them with the predictions. The topics to be analyzed include:

- Neutron flux measurements in the central rod above the spallation zone, at the neutron beam ports and in the two-irradiation stations are used to verify the MCNPX and FLUKA calculations and benchmark neutron yields (see Section 9.3 gives already evaluation of first results).
- The system behaviour re-assessment and comparison with model predictions. The heat transfer characteristics of the target heat exchanger will be analyzed in detail.
- The beam window cooling has been simulated using CFD. Temperature measurements close to the beam entrance window will be evaluated to conclude on the validity of the models.
- The overall system behaviour over 4 months of operation will be analyzed and the performance and degradation of individual components will be assessed.
- The data collected during operation will be processed and stored and made available for other evaluations on request.

The plan on post irradiation experiments on containment materials will be shortly recalled in Section 9.4.

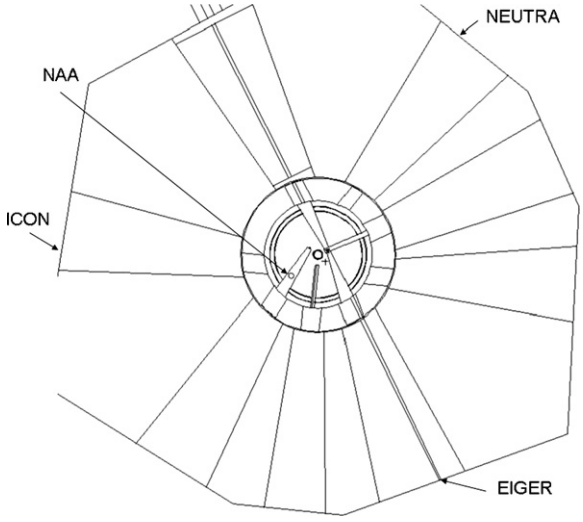

Fig. 19. Neutron flux measurement positions in the MCNPX model. A *XY* cut of the model at $Z = -18$ cm is shown. Collimators are included for the ICON, NEUTRA and EIGER beam lines (the ICON and NEUTRA collimators are at different longitudinal positions).

9.3. Neutronics evaluation during irradiation

9.3.1. Target performance compared with solid target

The performance studies made during the design work, as described in Section 4, showed the improvement of the MEGAPIE target with respect to the conventional solid target used at SINQ. During the MEGAPIE irradiation, a new campaign of simulations started to calculate the neutron fluxes at the actual positions were the measurements are performed (Fig. 19). In addition isotope production due to the spallation reaction have been as well measured and re-evaluated with a computational analysis. First results being extracted from the measurement program during irradiation are given in the following.

In Table 3 measurements of absolute thermal neutron fluxes in the beam lines at the exit from the SINQ target shielding block (about 6 m from the centre of the target) and at the NAA station (at about 80 cm from the center of the target) are shown. The measurement points are indicated in Fig. 19.

Results for the solid target used in 2004–2005 are also included in Table 3. The data show that: (i) the agreement between absolute flux values is rather good for most of the measurements. This indicates that the fluxes with the MEGAPIE target model are correctly calculated; and (ii) the measured

Table 3
Preliminary calculations and measurement values for relevant thermal neutron flux measurements ($n/cm^2/(s\ mA)$) with the MEGAPIE target (2006) and SINQ target 6 (2005)

	SINQ target 6 (2005)		MEGAPIE (2006)		RATIO	
	Experimental	Calculated ($E<1$ eV)	Experimental	Calculated ($E<1$ eV)	Experimental	Calculated ($E<1$ eV)
NEUTRA (30)	2.59×10^7 (8%)	2.45×10^7 (1%)	4.80×10^7 (5%)	3.85×10^7 (.5%)	1.85	1.57
ICON (50)	3.80×10^8 (8%)	4.59×10^8 (1%)	6.89×10^8 (7%)	7.70×10^8 (.5%)	1.81	1.68
EIGER (82)	6.47×10^8 (5%)	7.48×10^8 (1%)	1.04×10^9 (5%)	1.51×10^9 (.5%)	1.60	2.02
NAA	5.82×10^{12} (8%)	6.31×10^{12} (1%)	1.05×10^{12} (9%)	1.12×10^{13} (.1%)	1.80	1.77

Calculated values are the integral between 0 and 1 eV. Uncertainties are indicated in parentheses.

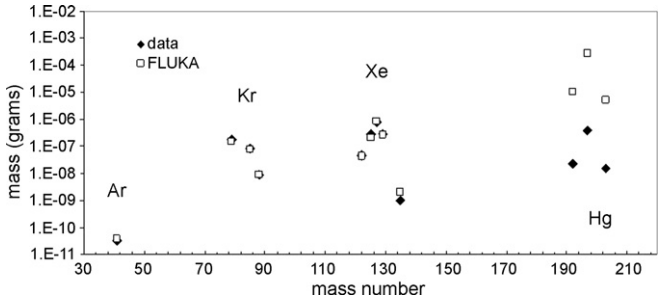

Fig. 20. Measured and calculated masses (FLUKA). ^{41}Ar, ^{79,85m,88}Kr, ^{122,125,127,129m,135}Xe and ^{192,197,203}Hg.

increase of the flux performance is of a factor 1.76, which is higher than the performance predicted for an "ideal" solid target. The difference is mostly understood in light of the newer calculations of the solid target, which include the STIP samples and the fact that the lead occupies 90% of the volume inside a rod; therefore it is possible to reproduce the measured improvement of the performance with the MEGAPIE target: the average calculated performance improvement is of a factor 1.75 which compares well with the average measured performance.

9.3.1.1. Gas production. The first results from the measurement of the gas samples produced following the spallation reaction are also available. In this case we are interested in estimating the amount of gas that is released at the beginning of the experiment. A gamma spectroscopy measurement from gas samples taken at the end of the second day of irradiation (after a total accumulated charge of 1 mA h) was performed. From this gas sampling, several noble gases and mercury radioisotopes were identified and the amount of the released radioisotopes was thus obtained. It is important to note that only a partial release is expected even for the noble gases on a short time scale.

The production of these isotopes was calculated using FLUKA (version 2006). The first results from this analysis are shown in Fig. 20. The dilution factor (that is, the fraction of gas in the MEGAPIE expansion volume that is sampled) is not precisely known yet and preliminary estimates indicate that overall the measured amounts are between 1% and 10% of the calculated values. This would correspond to a release of noble gases from the LBE between 1% and 10% after 2 days of operation. In the figure the data have been normalized to the calculated values for the noble gases, the normalization factor being the ratio between the sum of the calculated masses of Ar, Kr and Xe isotopes and the sum of the measured values. With this global normalization, it is apparent from the figure that there is a good agreement for all the individual isotopes of the three noble gas elements. On the contrary, the fraction of Hg isotopes that are released is very small: the release of Hg compared to the calculated value is about 500 times lower than for the noble gases.

Mass spectroscopy measurements from subsequent gas samples will hopefully allow us to measure the production of stable hydrogen and helium isotopes, as well as of tritium, which are

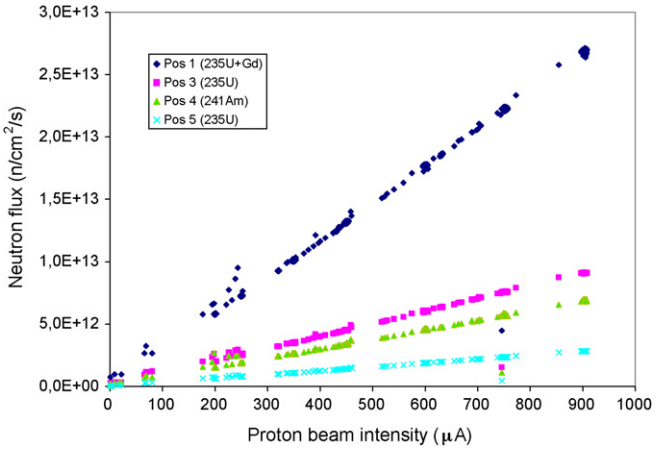

Fig. 21. Measured neutron fluxes as a function of the proton beam intensity, in different positions inside the central rod (see Section 4).

produced in larger quantities but cannot be measured by gamma spectroscopy.

From these results, and subsequent analyses, it will be possible to extract information on the relative production of the different isotopes and compare with the Monte Carlo predictions. The productions will be calculated, for the actual irradiation history, with different codes and spallation/evaporation models; the mass distribution of the measured release rates is strongly model dependent, and it is expected to benchmark the codes from these data.

9.3.2. Fission chambers results

The inner neutron flux was measured and monitored during the whole target irradiation with accuracy better than 5%. Preliminary results, for all the fission chambers (background subtracted), are shown in Fig. 21 as a function of beam intensity. These data have been recorded during the third phase of the start-up operation. As expected for such a system, the neutron flux is linearly correlated with the proton beam intensity. Moreover, the flux is higher at the lowest position (pos 1) than at the upper one (pos 5), as expected from simulations. Experimental data are in better agreement with the results of a new campaign of simulations than with the previous one, used to design the target. Among all the important improvements, the most sensitive for the inner neutronics simulation is the inclusion of boron (thermal neutron absorber) in the lead–bismuth eutectic composition, which was not present in the first simulations. More detailed analyses are in progress to extract the thermal/epithermal ratio.

9.4. Post irradiation experiments (PIE) of MEGAPIE containment materials

As already discussed in Section 4 the target components were fabricated of T91 and AISI 316L steels. By the end of irradiation, the MEGAPIE target has received about 3 A h proton charge, which corresponds at the beam window to a peak proton fluence of about 2×10^{25} p/m^2 and a maximum irradiation dose in the order of 8 dpa. During the MEGAPIE

irradiation, the target materials are exposed simultaneously to a relatively high dose and to flowing LBE, representing a unique condition.

The PIE of MEGAPIE includes surface inspections, microstructural examinations, chemical analysis, and mechanical tests. Surface inspections will be performed for studying LBE corrosion of the steels by means of optical microscopy, scanning electron microscopy, electron probe microanalysis etc. Microstructural examinations will be done to get information of microstructural changes induced by irradiation using transmission electron microscopes. Chemical analyses will also include radiochemical analyses using ICPMS, XRD, γ- and α-spectrometry techniques to reveal both radioactive and non-radioactive elements. Mechanical tests will be such tensile, bending and small punch tests to evaluate the degradation in mechanical properties caused by irradiation and LBE corrosion and embrittlement.

The PIE will be carried out by a joint effort of all the MEGAPIE partners and will start in 2009 when the samples are extracted from the components in hot-cells at PSI.

10. Summary and conclusion

The very challenging milestone to operate a representative, high power heavy liquid metal spallation target on the road towards a possible ADS development has been effectively achieved. Indeed, the MEGAPIE target, which is of significant power, has been operated successfully from August 2006 to December 2006 in the SINQ facility at PSI. The European Commission has supported the MEGAPIE initiative through the MEGAPIE-TEST project producing innovative know-how and expertise on the different components and materials of a heavy liquid metal spallation target. In this context the MEGAPIE-TEST consortium has gained a large experience to work at a multi-laboratory level and in a multi-disciplinary frame on a well-defined project. In fact, an important experience has been gained in structuring the collaboration between a design team and R&D multi-disciplinary teams active in different laboratories of different countries, in particular in order to face technical challenges and solve safety and licensing issues related to the experiment.

In Europe there is already a wide knowledge in the area of heavy liquid metal technology, as it is reported e.g. in the OECD/NEA (2007). With the MEGAPIE experiment, this knowledge has been enlarged to the assessment of an innovative heavy liquid metal system under irradiation in a proton field, which represents a relevant milestone for the development of HLM nuclear systems.

The results achieved so far within the MEGAPIE project, clearly indicate that a step forward has been made in the neutronics and thermal-hydraulics code validation for HLM systems. Moreover, an increased confidence has been gained in the procedures needed to assess structural material performances, in the area of component (e.g. pump systems) testing and on the crucial issue of the beam window coolability.

The activities and results obtained during the integral test and the irradiation phase of MEGAPIE are valuable from a scientific, operational and organisational point of view. For instance, the first analysis of the neutronics data gathered during the irradiation of MEGAPIE has already confirmed the calculations performed during the design phase. In fact, as expected an increase in neutron flux is obtained with the MEGAPIE target with respect to the performance of previous solid targets irradiated in SINQ.

Moreover, the integration of the target and of the ancillary systems, the execution of the integral test, the first operation and the irradiation, allowed getting confidence with the start-up and routine operation of this innovative system.

The next steps of the MEGAPIE project will be a comprehensive analysis and interpretation of the data collected during irradiation. This activity will be performed within the 6th Framework Programme EUROTRANS.

Furthermore, after the dismantling of the target, an extensive PIE is foreseen to complete the evaluation on the components and materials performance under irradiation completing the assessment of a first-of-a-kind high power liquid metal spallation target.

Acknowledgements

This work has been performed in the context EU-programs FIS5-2001-00090 with the acronym MEGAPIE-TEST

References

AAA Materials Handbook, 2003. Materials data for particle accelerator applications TPO-P00-Z-MDD-X-00001; LA-CP-01-0168; Revision 3.

Agostini, P., Baicchi, E., Zucchini, A., Benamati, G., 2004. The re-crystallization issue in lead-bismuth technology. J. Nucl. Mater. 335, 275–279.

Aiello, A., Agostini, M., Benamati, G., Long, B., Scaddozzo, G., 2004. Mechanical properties of martensitic steels after exposure to flowing liquid metals. J. Nucl. Mater. 335, 217.

Arien, B., 2003. ASCHLIM: a 5th FP Project for the Assessment of CFD Codes Applied to Heavy Liquid Metals, International Workshop on P&T and ADS Development, SCK CEN, Mol, Belgium, pp. 6–8.

Agostini, P., Baicchi, E., 2002. Observations resulting from MEGAPIE cooling pin tests in Brasimone, ENEA Report MP-T-R-001. Brasimone 27.08.2002.

Auger, T., Lorang, G., Guérin, S., Pastol, J.-L., Gorse, D., 2004. Effect of contact conditions on embrittlement of T91 steel by lead–bismuth. J. Nucl. Mater. 335, 227.

Bauer, G.S., Salvatores, M., Heusener, G., 2001. MEGAPIE, a 1 MW pilot experiment for a liquid metal spallation target. J. Nucl. Mater. 296, 17–33.

Buchenau, D., Eckert, S., Gerbeth, G., 2006. Status of the measurement techniques development, IP-EUROTRANS-DEMETRA Deliverable D4.13. EU-Contract No. FI6W-CT2005-516520.

Buono, S., Maciocco, L., Moreau, V., Sorrentino, L., 2001. Thermal-hydraulic analysis of the MEGAPIE Manifold, CRS4-TECH-REP-01/117.

Buono, S., Maciocco, L., Moreau, V., Sorrentino, L., 2002. Optimisation of the pin cooler design for the megapie target using full 3D numerical simulations, CRS4-TECH-REP-02/3.

Cadiou, A., 2004. Megapie design & analysis. Technical Review Meeting, Mol, Belgium, June 28–30, 2005.

Chabod, S., et al., 2006. Neutron flux characterization of the MEGAPIE target. NIMA5662 (2006) 618.

Chen, H., Cheng, X., 2005. ATHLET-MF-code and its application to HLM cooled systems. FZKA Report, FZKA-7165.

Corsini, G., Dubs, M., Sigg, B., Wagner, W., 2003. Heat removal system: final update of concept and detail design, dimensional and functional issues. In:

Proceedings of the 4th MEGAPIE Technical Review Meeting, FZKA-6876, p. 34.

Dai, Y., Henry, J., Auger, T., Vogt, J.-B., Almazouzi, A., Glasbrenner, H., Gröschel, F., 2006. Assessment of the lifetime of the beam window of Megapie target liquid metal container. J. Nucl. Mater. 356, 308.

Dai, Y., 2004. Irradiation under neutron-proton mixed spectrum in SINQ targets and related post-irradiation examination. PSI report TM-34-04-08.

Daubner, M., Batta, A., Fellmoser, F., Lefhalm, C.-H., Mack, K.-J., Stieglitz, R., 2004. Turbulent heat mixing of a heavy liquid metal flow within the MEGAPIE window geometry—The HEATED JET Experiments. J. Nucl. Mater. 335, 286–292.

Daubner, M., Batta, A., Fellmoser, F., Lefhalm, C.-H., Stieglitz, R., 2005. Turbulent heat mixing of a heavy liquid metal flow in a target window geometry—The Heated Jet Experiment. FZKA-7098.

Dementjev, S., Gröschel, F., Ivanov, S., Platacis, E., Von Holzen, G., Zik, A., 2003. EMPS for MEGAPIE target. Testing of the Prototype. PSI-Report MPR-11-DS34-005/0.

Dementjev, S., Gröschel, F., Ivanov, S., Ming, P., 2005. Thermal-hydraulics test of the MEGAPIE electro magnetic pump system in LBE. PSI-Report MPR-11-DS34-036.

Dementjev, S., Barbagallo, F., Groeschel, F., Heyck, H., Joray, S., Patorski, J., 2006. Integral test of the MEGAPIE target at MITS. PSI Report MPR-11-DS34-094, April 2006.

Duperrex, P.-A., Müller, U., 2006. Target E transmission measurements for Megapie. PSI TM 84-06-02, p. 26.

Dury, T.V., 2003a. CFD design support at PSI for the international MEGAPIE liquid–metal spallation target. In: Proceedings of the International Conference on Nuclear Engineering (ICONE-11), Tokyo, Japan, April 20–23 (CD-ROM).

Dury, T.V., 2003b. CFD simulation of focused-beam transient. Proceedings of the 4th MEGAPIE Technical Review Meeting, Paris, March 18–19, 2003. FZK Scientific Report, FZKA 6876, pp. 79–82.

Enderlé, R., Klein, K.K., 2001. Compilation of results of the neutronic benchmark on the MEGAPIE spallation target, SERMA/LCA/RT/01-3027/A.

Enqvist, T., et al., 2001. Nucl. Phys. A 686, 481.

Fassò, A., et al., 2001. In: Lisbon, A., Kling, F., Barao, M., Nakagawa, L., Tavora, P.Vaz. (Eds.), Proceedings of the Monte Carlo 2000 Conference. Springer-Verlag, Berlin, p. 159.

Fazio, C., Alamo, A., Almazouzi, A., Gomez-Briceno, D., Groeschel, F., Roelofs, F., Turroni, P., Knebel, J.U., 2005. Assessment of Reference structural materials, heavy liquid metal technology and thermal-hydraulics for European waste transmutation ADS. In: Proceedings of the GLOBAL 2005 Conference, Tsukuba, Japan, October 9–13.

Freibergs, E., Platacis, E., 2002, Electro-magnetic pump system—a detailed design. Institute for Physics Report IPUL 1069.00.00-05.

Freibergs, E., Platacis, E., 2003. EMP system for PbBi melt at 280–450 °C. Institute for Physics Report, February 20, 2003.

Freibergs, E., Platacis, E., 2006. Calibration tests of electromagnetic flow meters of EMPs on the Riga Stand and MITS; IPUL Report IPMP-EMP-IF-070-1.

Henry, J., Lamagnère, P., 2003. Risk of failure of the Pb–Bi container window: a tentative assessment. CEA report DMN/SRMA/LA2M/NT/2003-2585, and FzK report FZKA 6876, Forshingszentrum Karlsruhe, 184.

Ivanov, S., Platacis, E., Flerov, A., Zik, A., Ming, P., Groeschel, F., Dementjev, S., 2006. Experience of calculation, design, fabrication and testing of the electromagnetic pump system for the MEGAPIE target. Magnetohydrodynamics 42 (2/3), 275–280.

Ivanov, S., Dementjev, S., 2006. Temperature monitoring of the lead–bismuth eutectic flow in the MEGAPIE target. Magnetohydrodynamics 42 (2/3), 281–289.

Jekabsons, N., 2006a. MEGAPIE TARGET development of an alternative flowrate measurement system in bypass contour of MEGAPIE TARGET. Report JESMPTARGNJ-002/0.

Jekabsons, N., 2006b. Considerations on MEGAPIE target electromagnetic flowmeters calibration and further operation. PAIC report PAIC-MP-EMP-NJ-008, Riga.

Kalkhof, D., Grosse, M., 2003. Influence of PbBi environment on the low-cycle fatigue behavior of SNS target container materials. J. Nucl. Mater. 318, 143.

Lefhalm, C.-H., Gnieser, S., Stieglitz, R., 2005. Velocity measurements witihn a beam window geometry. Jahrestagung Kerntechnik Nürnberg 2005; Inforum GmbH.

Leung, W.H., 2004. On the MEGAPIE target thermal hydraulics—a RELAP5 analysis. In: Proceedings of ICONE 12, Paper Nr. 49378, Arlington, Virginia, USA, April 25–29.

Leung, W.H., 2006. MEGAPIE-Technical Review Meeting, Villigen-PSI, Switzerland, March 23–24, 2006.

Leung, W.H., 2005. Thermal-hydraulic system behavior and the target temperature regulation. In: MEGAPIE Technical Review Meeting, Mol, Belgium, June 28–30.

Meloni, P., Casamirra, M., Castiglia, F., Giardina, M., 2006. Validation of RELAP5 heat trasnfer correlation on single pin and MITS tests. In: Proceedings of the 7th MEGAPIE Technical Review Meeting, PSI, Switzerland, May 28–31.

Nicaise, G., Legris, A., Vogt, J.B., Foct, J., 2001. Embrittlement of the martensitic steel 91 tested in liquid lead. J. Nucl. Mater. 296, 256.

OECD/NEA, 2007. Handbook of Pb–Bi Eutectic Alloy and Pb Properties, Materials Compatibility, Thermal-Hydraulics and Technologies.

Patorski, J., Bauer, G., Platnieks, I., Takeda, Y., 2000. Experimental estimation of optimum Bypass-jet-flow conditions for the cooling of the window of the SINQ liquid metal target, PSI Report 2000, vol. VI, pp. 42–44 (ISSN 1423-7350, PSI, CH-5232 Villigen, Switzerland).

Patorski, J., Sigg, B., Platnieks, I., Groeschel, F., Stieglitz, R., 2004. Results of IRT- & TC KILOPIE-1 Experiments; PSI Scientific. Report 2004.

Perret, C., 2002. Sicherheitsbericht zum Megapie-Experiment an einem Target mit Blei-Bismut-Eutektikum in der Neutronenquelle SINQ des PSI, Safety Analysis Report, June 2002.

Petrazzini, M., Alemberti, A., 2002. Thermal hydraulic analysis report. Ansaldo report MPIE 1 TRIX 201, Genova, Italy.

Rohrer, U., 2001. A novel method to improve the safety of the planned MEGAPIE target at SINQ, PSI Scientific and Technical Report 2001, vol. VI, pp. 34–35.

Roubin, P., 2004. MEGAPIE steady-state simulation of the lower target thermal hydraulics: final optimisation of the nozzle geometry, CEA Document SMTM/LMTR/2004-07, 2004.

Roubin, P., 2001. MEGAPIE steady state simulation of the lower target thermal-hydraulics. Preliminary cases without heat source in the structures. CEA-NT DEN/DTP/STH/LTA/2001-12.

Roubin, P., 2002. MEGAPIE steady state simulation of the lower target thermal-hydraulics. Cases without Bypass (Benchmark M1). CEA-NT DEN/DTP/STH/LTA/2002-17.

Roubin, P., 2003. MEGAPIE steady state simulation of the lower target thermal-hydraulics. Cases with Bypass and reference nozzle geometry. CEA-NT DEN/DTP/STH/LTA/2003-3.

Roubin, P., 2003. MEGAPIE steady state simulation of the lower target thermal-hydraulics. Optimization of the nozzle geometry. CEA-NT DEN/DTP/STH/LTA/2003-25.

Salvatores, M., et al., 1994. A global physics approach to transmutation of radioactive nuclei. Nucl. Sci. Eng. 116, 1.

Salvatores, M., 2005. Nuclear fuel cycle strategies including partitioning and transmutation. Nucl. Eng. Des. 235, 805.

Samec, K., 2006. Full scale leak test of the MEGAPIE containment hull, PSI External Report, 06-02, July 2006.

Samec, K., 2003. Parametric study of the insulation barrier on the lower target enclosure PSI internal document TM-34-03-14, November 2003.

Smith, B.L., Dury, T.V., Maciocco, L., Roubin, P., Tak, N.I., 2003. A benchmark study based on a representative design of the MEGAPIE spallation source target. In: Proceedings of the 10th International Topical Meeting on Nuclear Reactor Thermal Hydraulics (NURETH-10), Seoul, Korea, October 5–9, 2003 (CD-ROM).

Smith, B.L., Dury, T.V., Ni, L., Zucchini, A., 2004. A pragmatic coupling strategy between commercial CFD and structure analysis code. In: Proceedings of the 5th International Symposium on Computational Technologies for Fluid/Thermal/Chemical/ Stressed Systems with Industrial Applications, vol. 491-1, San Diego, USA, July 24–28, 2004, pp. 101–109.

Smith, B.L., Leung, W.H., Zucchini, A., 2005. Coupled fluid/structure analyses of the MEGAPIE spallation source target during transients. In: Proceed-

ings of the 11th International Topical Meeting on Nuclear Reactor Thermal Hydraulics (NURETH-11), Paper 509, Avignon, October 2–6,2005.

Smith, B.L., 2006, Summary report for MEGAPIE R&D task group X4: fluid dynamics and structure mechanics, PSI External Report, 06-01, March 2006.

Smith, B.L., 2002, Summary of the first MEGAPIE-CFD benchmark study PSI-Internal Report MPBE-4-BR-1/0, 2002.E.

Smith, B.L., Shepel, S.V., 2005. CFD Analysis of a Possible Leakage of Coolant in the MEGAPIE Spallation Source Target, Proc. ASME Heat Transfer Conference and Interpack'05, 17–22 July 2005, San Francisco, USA, CD-ROM (ISBN 0-7918-3762-9).

Stieglitz, R., 2003, MHD-features of the main service and bypass pump in the MEGAPIE design. FZKA Report FZKA-6826.

Stieglitz, R., Zeininger, J., 2005. A 2D model to design MHD induction pumps. In: Proceedings of the 6th International Pamir Conference, vol. 2, Jurmala Latvia, pp. 140–153.

Tak, N.-I., Cheng, X., 2001. Numerical design of the active part of the MEGAPIE target, FZKA-Report 6611, May 2001.

Thomsen, K., 2005. VIMOS, a novel visual device for near-target beam diagnostics, ICANS-XVII. In: Proceedings of the 7th Meeting of the International Collaboration on Advanced Neutron Sources, Santa Fe, New Mexico, April 25–29, 2005.

Thomsen, K., 2006a. Test plan for the MEGAPIE safety systems, MEGAPIE document MPR-3-193/4, August 10, 2006.

Thomsen, K., Schmelzbach, P., 2006. Report on beam safety systems for MEGAPIE, MEGAPIE document MPR-3-TK34-167/3, February 24, 2006.

Thomsen, K., 2006b. LBE leak detectors for MEGAPIE, MEGAPIE document MPR-3-TK34-181/2, February 13, 2006.

Turroni, P., 2005, Megapie project fill and drain system—functional description. ENEA Report FIS-P817-001, rev.1, 04/03/05.

Van den Bosch, J., Sapundjiev, D., Al Mazouzi, A., 2006. J. Nucl. Mater. 356, 237–246.

Vogt, J.B., Verleene, A., Serre, I., Balbaud-Célérier, F., Terlain, A., September 2005. Coupling effects between corrosion and fatigue in liquid Pb–Bi of T91 martensitic steel. In: Proceedings of the Eurocorr 2005, Lisbonne.

Wagner, W., Groeschel, F., Corsini, G., 2003a. Cover gas system: updated boundary conditions and current concept. In: Proceedings of the 4th MEGAPIE Technical Review Meeting, FZKA 6876, p. 40.

Wagner, W., Turroni, P., Agostini, P., Thomsen, K., Wagner, E., Welte, J., 2003c. Fill and drain and freezing: system modifications for merely non-active draining. In: Proceedings of the 4th MEGAPIE Technical Review Meeting, FZKA 6876, p. 46.

Wagner, W., Welte, J., Joray, S., Sigg, B., 2003b. Insulation gas system of MEGAPIE: a concept update. In: Proceedings of the 4th MEGAPIE Technical Review Meeting, FZKA 6876, p. 52.

Waters, L.S., et al., 2002. MCNPX Users's Manual Version 2.4.0, LA-CP-02-408.

Zanini, L., 2005. Summary Report for MEGAPIE R&D Task Group X9: Neutronic and Nuclear Assessment, PSI Bericht Nr. 05-12, ISSN 1019-0643.

Zanini, L., et al., 2005. International conference on nuclear data for science and technology. In: Haight, R.C., Chadwick, M.B., Kawano, T., Talou, P. (Eds.), AIP Conference Proceedings, vol. 769. Melville, New York, p. 1525.

Zucchini, A., Agostini, P., Baicchi, E., 2005. Lead–bismuth eutectic recrystallization studies for the megapie target. J. Nucl. Mater. 336, 291–298.

Zucchini, A., 2002a. MEGAPIE: target stresses due to LBE expansion after solidification, RT/2002/49/FIS, ENEA, 2002.

Zucchini, A., 2002b. MEGAPIE: stress analysis of lower target preliminary design. RTI/FIS/MET/2002/1, ENEA, 2002.

Zucchini, A., 2004. MEGAPIE: 3-D Simulations of lbe expansion in the target after solidification. RTI/FIS/MET/2004/1, ENEA, 2004.

Zucchini, A., Smith, B.L., 2003a. Stress analysis of the LMC under accident conditions. In: Proceedings of the of the 4th MEGAPIE Technical Review Meeting, Paris, March 18–19, 2003, FZKA 6876, pp. 87–92 (FZK 2003).

Zucchini, A., Smith, B.L., 2003b. Stress analysis of LMC under normal operating conditions. In: Proceedings of the of the 4th MEGAPIE Technical Review Meeting, Paris, March 18–19, 2003, FZKA 6876, pp. 131–133 (FZK 2003).

Zucchini, A., Agostini, P., Baicchi, E., 2003. Pb–Bi eutectic recrystallization studies for MEGAPIE target. In: Proceedings of the 4th MEGAPIE Technical Review Meeting, Paris, March 18–19, 2003, FZKA 6876, pp. 244–256 (FZK 2003).

Zucchini, A., 2005. Overview of structural analysis results in support of the target design. In: Proceedings of the 5th MEGAPIE Technical Review Meeting, Nantes, May 24–26, 2004, pp. 299–306 (Subatech, 2005).